NASA TECHNICAL NOTE

NASA TN D-6421

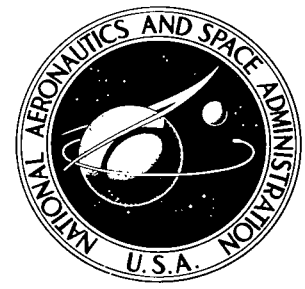

VALIDATION OF SERT II THERMAL ANALYTICAL TECHNIQUES BY THERMAL VACUUM TESTING OF THE PROTOTYPE SATELLITE

by George R. Smolak and N. John Stevens

Lewis Research Center
Cleveland, Ohio 44135

NATIONAL AERONAUTICS AND SPACE ADMINISTRATION • WASHINGTON, D. C. • NOVEMBER 1971

1. Report No.	2. Government Accession No.	3. Recipient's Catalog No.
NASA TN D-6421		

4. Title and Subtitle	5. Report Date
VALIDATION OF SERT II THERMAL ANALYTICAL TECHNIQUES BY THERMAL VACUUM TESTING OF THE PROTOTYPE SATELLITE	November 1971
	6. Performing Organization Code

7. Author(s)	8. Performing Organization Report No.
George R. Smolak and N. John Stevens	E-6396
	10. Work Unit No. 704-13

9. Performing Organization Name and Address	11. Contract or Grant No.
Lewis Research Center National Aeronautics and Space Administration Cleveland, Ohio 44135	
	13. Type of Report and Period Covered: Technical Note

12. Sponsoring Agency Name and Address	14. Sponsoring Agency Code
National Aeronautics and Space Administration Washington, D.C. 20546	

15. Supplementary Notes

16. Abstract

The thermal protection system for the flight configuration of the SERT II satellite was designed using an analytical thermal network to represent the satellite and its environment. A large part of this digital analytical network was adjusted and calibrated by comparing predicted temperatures with experimental measurements made with the prototype SERT II satellite in an extended thermal vacuum test. This report outlines the procedures used in adjusting and calibrating the analytical network.

17. Key Words (Suggested by Author(s))	18. Distribution Statement
Spacecraft Satellite design Thermal vacuum test Thermal protection Thermal analysis Thermal mathematical model	Unclassified - unlimited

19. Security Classif. (of this report)	20. Security Classif. (of this page)	21. No. of Pages	22. Price*
Unclassified	Unclassified	47	$3.00

* For sale by the National Technical Information Service, Springfield, Virginia 22151

VALIDATION OF SERT II THERMAL ANALYTICAL TECHNIQUES BY THERMAL VACUUM TESTING OF THE PROTOTYPE SATELLITE

by George R. Smolak and N. John Stevens

Lewis Research Center

SUMMARY

The thermal protection system for the flight configuration of the SERT II satellite was designed using an analytical thermal network to represent the satellite and its environment. A large part of this digital analytical network was adjusted and calibrated by comparing predicted temperatures with experimental measurements made with the prototype SERT II satellite in an extended thermal vacuum test. This report outlines the procedures used in adjusting and calibrating the analytical network.

INTRODUCTION

The second Space Electric Rocket Test (SERT II) satellite was designed to life test either of its two 1-kilowatt mercury-bombardment ion thrusters in a space environment for a minimum of 6 months. In its orbiting configuration (fig. 1) the SERT II satellite comprises the Agena D vehicle with its forward equipment rack, a spacecraft support unit (SSU) which houses the command system, telemetry, and control moment gyros, (CMG's), and the spacecraft (S/C) which houses two ion thrusters and associated experiments. The satellite was launched on February 3, 1970 into a circular, near-polar orbit with an initial altitude of 1000 kilometers (540 n mi). The satellite is gravity gradient stabilized and does not spin. Therefore, the same cylindrical side of the satellite always faces the sun. Details of the SERT II mission can be found in reference 1.

A thermal control system was required for the SERT II satellite to satisfy the temperature constraints on many electrical components while accounting for large variations expected during the mission in internal power dissipation and external radiation environment. Preliminary analyses indicated that the most difficult temperature constraints to satisfy were those pertaining to an internal battery and a power conditioner package mounted on a shade-side radiator plate. Several alternatives for designing the flight

thermal control system were considered. It was decided that the flight thermal control system (ref. 2) would be designed using an analytical model based on techniques used to predict temperatures in the SERT II prototype satellite during a thermal-vacuum test sequence.

For this thermal-vacuum test sequence the prototype satellite was equipped with extensive temperature instrumentation. Solar simulation was not a part of these tests. Temperatures from these tests were compared to the analytical results for both steady state and transient conditions. The analytical model was then modified (iteratively) to improve the agreement.

The purpose of this report is to present in detail the analytical techniques used in setting up the prototype SERT II satellite thermal model and the methods used in changing the model to improve the agreement with experimental data. Comparisons between the final analytical results and the experimental temperatures are presented.

NOMENCLATURE

BACS	backup acquisition system
CMG	control moment gyro
CONFAC	configuration factor
FM	frequency modulated
MESA	miniature electrostatic accelerometer experiment
PCM	pulse code modulated
PM	phase modulated
REX	reflector erosion experiment
RFI	radiofrequency interference experiment
S/C	spacecraft
SERT	Space Electric Rocket Test
SMR	switching mode regulator
SSU	spacecraft support unit
TC	thermocouple
TM	thermistor
α_s	solar absorptance
ϵ	emittance

APPARATUS

The prototype version of the SERT II satellite was subjected to a thermal-vacuum qualification test in a space environmental test chamber at the NASA Lewis Research Center (ref. 3). A portion of the thermal results from that test is the basis for this report.

Figure 2 shows the spacecraft (S/C), spacecraft support unit (SSU), and Agena simulator as they were installed in a space environment test chamber at the NASA Lewis Research Center. Cables were used to suspend the test specimen with the longitudinal axis in a horizontal position. A large solar simulator was not available for these tests. Instead, the sun-side skins (bays 1, 7, and 8) of the S/C and SSU (fig. 2(b)) were heated by radiation from a concentric "variable heating panel" spaced close to the skins. This heating panel also radiated to a portion of the top covers of the S/C. The heat sink for the satellite was liquid nitrogen cooled cold walls surrounding the specimen. An uncooled contamination shield was positioned normal to the satellite axis to intercept sputtered particles from the ion thruster and/or shield which would have contaminated the S/C and SSU. The shield diameter was 4.57 meters (15 ft) to fill the test chamber. The center 1.83-meter (6-ft) diameter was solid metal and the remainder was open mesh screen. Auxiliary lamps were positioned to provide heating for the thruster and power conditioner radiator during certain nonoperating periods to prevent excessive cooldown of these components. The Agena simulator (i.e., an Agena transition ring with a diaphragm attached) was mounted with shims to the base of the SSU in a manner similar to the flight configuration. The temperature of the simulator was adjusted with four sets of strap-on electrical heaters. A radiation barrier consisting of multiple layers of aluminized mylar covered the base of the Agena simulator ring much as the Agena "forward wall" would do in space.

The S/C and SSU basic structures were bolted and riveted as shown in figures 3(a), (b), and (c). Components were bolted to trays (figs. 3(d) and (f)). The structure was predominantly aluminum alloy with some parts magnesium alloy. An effort was made to ensure good conduction of heat in the structure (through joints, between components and trays, and between skins and structure) by generous use of fasteners and ample material thicknesses. Indium foil was used only in mounting several critical components (power conditioner, for example) to the structure.

The prototype configuration of the S/C (fig. 4) and the SSU (fig. 5) differed from the flight configuration (figs. 3(d), (e), and (f)) in that several major flight experiment components were missing. Reference 1 contains a description of the SERT II experiments and mission. There was an ion thruster in bay 6 only of the S/C. The corresponding bay 2 thruster was not installed. Instead an aluminum cover plate similar to the covers on bays 1, 7, and 8 was put over the top of this bay. The matching power conditioner

package for the bay 2 thruster was also omitted from the test specimen. The flight radiofrequency interference experiment (RFI) antenna, reflector erosion experiment (REX), and both contamination experiments (figs. 3(d), (e), and (f)) were omitted from the top of the S/C. Both the beam probe and the space probe were mounted on the test specimen. The four CMG's consisted of one prototype unit, one experimental unit, and two simulators. The analytical network representing the prototype satellite incorporated all of these just enumerated features.

Thermal instrumentation was installed on the satellite skins, bulkheads, trays, and components as shown in figures 4 and 5. The 35 thermistor installations corresponded to the flight configuration. Data from the thermistors were digitized and transmitted through the flight telemetry link (PCM/FM/PM system). Thermocouples were hard wired and mounted close to each thermistor to provide a check of the thermistor accuracies. In addition, thermocouples were located at a number of other points (for a total of 142 thermocouples) so that a more complete check of the analytical and experimental temperature agreement could be made.

The full environmental test program to which the prototype satellite was exposed consisted of six segments. For brevity, this report is restricted to segments 2 to 5 because they adequately demonstrate all the thermal techniques important to this document.

Segment 2 was a cooldown from room temperature which lasted from zero to 24 hours of "test time." The variable heater panel temperature was set at 49° C to simulate a high incident solar flux condition. Power dissipation to the structure (shown in table I and fig. 6) consisted of housekeeping, 105 watts, thruster, 90 watts, and power conditioner, 150 watts. The environmental chamber cold walls were gradually brought to liquid nitrogen (LN_2) temperature during this period. For the balance of the 97 hours of test time, the cold walls remained at LN_2 temperature.

For segment 3 (test time from 24 to 37 hr) the variable heater panel temperature was set at 32° C to simulate a lower incident solar flux than segment 2. Housekeeping, thruster, and power conditioner dissipations remained unchanged.

Segment 4 (test time from 37 to 48 hr) simulated a low power reacquisition sequence. The thruster lamps were on, and both the thruster and power conditioner units were off. Remaining power levels were emergency, 20 watts (37 to 39 hr), CMG's on, 40 watts (39 to 42 hr), and emergency, 20 watts (42 to 48 hr).

Segment 5 (48 to 97 hr) was a high power test with power dissipation at 110-watt housekeeping, 125-watt power conditioner, and thruster at 90 watts except for a temporary thruster-power conditioner shutdown from 68 to 72 hours. The variable heater panel temperature was set at 49° C as in segment 2.

ANALYSIS

A thermal control system was needed for the flight version of the SERT II satellite. It was decided that the design of such a system would be based on analytical techniques which would be applied to the prototype version of the SERT II satellite. These techniques would then be verified in a thermal-vacuum test of the prototype satellite. Because the satellite was large, complex, and densely packed, past experience with thermal modelling indicated that a several hundred node thermal network was required to demonstrate that the numerous thermal constraints could be satisfied.

An appraisal was made of available NASA and contractor digital computer programs which were both capable of handling thermal analysis of spacecraft and compatible with the NASA Lewis IBM 7094 computers. A General Dynamics "thermal analyzer" program (ref. 4) had been used successfully for preliminary analysis with relatively small networks. Many other programs, such as Lockheed's (ref. 5) and Chrysler's (ref. 6), were considered. The Chrysler Improved Numerical Differencing Analyzer (CINDA) program (ref. 6) was finally adopted because of its flexibility and capability for efficiently handling thermal network analysis.

Input for the CINDA program included information necessary to describe the lumped-parameter, thermal-analog network which was constructed to represent the satellite. Each of the 215 elements (nodes) in the network was separately identified and assigned a value for thermal capacitance (product of weight and specific heat) and initial temperature. The node network is indicated in figures 4 and 5. In general, dashed lines denote node boundaries. Judgement was applied in placing node boundaries along expected isotherms. However, components on all trays were lumped into a single component in the network. The effect of lumping components into a single node is generally to predict a high temperature for all the high power components. As illustrated in figures 3(a) to (f), there were numerous bolted and riveted connections (or joints) between bulkheads, angles, trays, skins, and channels. A thermal conductance value of 567 W/$(m^2)(^oC)$ or 100 Btu/(hr)$(ft^2)(^oF)$ was used for all S/C and SSU joints except between components and structure. This value was based on both unpublished experimental measurement of heat transfer across isolated joints and references 7 and 8. Conduction from the SSU to the Agena simulator through the Agena transition ring was based on a thermal network supplied by Lockheed. A total of 455 conductors were used in the network to represent the conduction in the satellite.

Two major classes of radiation were present in the thermal tests. First, there was a radiation interchange among surfaces inside the S/C and SSU structures. Highly emissive paint (emittance of 0.9) covered these surfaces to enhance the radiation. A total of 414 radiation conductors in the network to represent this mode of heat transfer were calculated either by hand or by use of a digital computer program called CONFAC II (ref. 9). The second class of radiation involved interchange of heat between

the external surfaces of the S/C and SSU (mostly aluminum foil tape having an assumed emittance of 0.06) and various surfaces around the suspended satellite (fig. 2). Here, also, the CONFAC II program was used to calculate view factors between the surfaces.

In the analytical program, the temperatures of nodes representing the skin surfaces of bays 1, 7, and 8 of both the S/C and SSU were controlled and treated as boundary temperatures for each time interval. Other boundary temperatures were the top covers on the center bay and bays 1, 7, and 8 of the S/C and the radiation barrier simulating the Agena forward wall.

Heat dissipation from internal components followed the profile shown in figure 6. The source of component dissipations was either vendor specifications or power dissipation test data.

The major uncertainties in the analytical model assumptions were the thermal capacitance of components and the conduction paths between components and structure.

RESULTS AND DISCUSSION

The thermal protection system for the flight configuration of the SERT II satellite was designed using an analytical thermal network to represent the satellite and its environment. A large part of this digital analytical network was adjusted and calibrated by comparing predicted temperatures with experimental measurements made with a prototype SERT II satellite in an extended thermal vacuum test. Thus, it was possible to extrapolate from the prototype satellite configuration and test environment to the flight satellite configuration and environment.

Without experimental data it was not possible to formulate an analytical network for the SERT II satellite which would have sufficient accuracy to satisfy the thermal design constraints. The chief reason for this was the uncertainty in the assumptions for (1) thermal capacitance of components, and (2) thermal conduction between components and the structure.

To improve transient temperature agreement, the thermal capacitance of components was adjusted as required. Similarly, to improve steady-state temperature agreement, the values used for the component to structure conductors were changed where necessary. Table II is a summary of both of these changes. No changes were made in the conduction model of the basic structure. The adjustment procedure was iterative and tedious. No automatic or optimization techniques were used in this process. Computerized optimization procedures are available (refs. 10 and 11) but they are generally restricted to small networks. Only the final agreement between analytical and experimental temperatures is presented in this report. These temperature presentations are divided into two major categories, spacecraft and spacecraft support unit.

Temperature Comparisons

Table III(a) is a summary of spacecraft structure, tray, and component temperatures. Final predicted (analytical) temperatures are compared qualitatively to adjacent thermocouple measurements for transient slope (good, fair, or poor) and quantitatively for steady-state level (in ^{o}C above and below thermocouple). The agreement between thermocouples and thermistors is given in the fourth column (^{o}C above and below thermistor). The fifth column in table III(a) indicates the figure number(s) from which the data in columns 2 to 4 were obtained. Averages have been given for each of the columns for both the structure and components. Temperature comparisons for the spacecraft support unit are given in table III(b). Typical transient and steady-state regions for table II are indicated in figure 7. In both the S/C and SSU the expected good agreement ($\pm 4^{o}$ C) between thermistors (telemetry link) and thermocouples (hard wired) established the level of accuracy of the flight thermistors.

Spacecraft. - The predicted temperatures for both the structure and components were within $\pm 4^{o}$ C of measurements (figs. 7 to 28) with several exceptions. These exceptions occurred for components in areas of either large power dissipation or large thermal capacitance where the lumped-node assumption for components was expected to be least accurate.

The temperature predicted for the bay 3 to 4 bulkhead (fig. 17) was as much as 5^{o} C below the thermocouple reading. This was probably caused by both the large temperature gradient from the immediately adjacent, hot, power conditioner package and the large node size in this area (fig. 4(b)).

The thruster was approximated with a single node in the analytical model even though it was known that large temperature differences existed between parts of operating thrusters. Fortuitously, figure 27 shows excellent steady-state agreement between the thruster arc chamber and this predicted single node temperature.

On the bay 8 upper tray (fig. 23) the largest heat dissipating components were the horizon sensor electronics and the space probe electronics. As expected, these components were warmer than other components on the same tray. The lumped component predicted temperature was warmer than any component measured temperature on this tray.

The miniature electrostatic accelerometer (MESA), MESA electronics, and RFI electronics were the largest heat dissipators on the bay 8 lower tray (fig. 24). The MESA and MESA electronics were even warmer than the lumped component predicted temperature.

Agreement between predicted and measured transient temperature slopes was generally good. Exceptions were fair agreement for the bay 4 bulkhead, MESA sensor and MESA electronics, and poor agreement for the thruster, as expected.

Spacecraft Support Unit. - The steady-state structure temperatures predicted for the spacecraft support unit were within $\pm 4^{\circ}$ C of the thermocouple measurements (table III(b) and figs. 29 to 53). Again, the analysis assumed a lumped single component instead of individual components.

Agreement between predicted and measured transient temperature slopes again was generally good. The only exception was the bay 4 upper tray, where only fair agreement was noted.

Evaluation of Analytical Techniques

The analytical techniques used to construct and improve a thermal model of the satellite were considered validated by comparison with the prototype thermal vacuum test results. Confidence was also gained in extrapolating these techniques from the prototype configuration and environment to design of the thermal control system for the flight configuration and environment.

Several iterations (involving changing component thermal capacitances and component to structure thermal conduction) were necessary to arrive at the final agreement between analytical and experimental temperatures shown in table III. The only optical property iteration in the analysis involved the emittance of the aluminum foil tape. The final value used was an emittance of 0.06. Because the bay 1, 7, and 8 skin temperatures were boundary temperatures, iteration of emittance on these surfaces was not meaningful. Computer plots of analytical and experimental temperatures against time were found to be quite helpful in guiding the iterative efforts.

CONCLUDING REMARKS

Thermal analytical techniques for the prediction of steady-state and transient temperatures of the prototype SERT II satellite were successfully validated by comparison with thermal vacuum test results. Confidence was gained that these analytical techniques could be applied to the design of the thermal control system for the flight version of the SERT II satellite.

An iterative method of adjusting unknown factors (electronic package thermal capacitances and electronic package to structure conductions) in an analytical network to

improve the agreement between predicted and measured temperatures was highly successful.

Lewis Research Center,
National Aeronautics and Space Administration,
Cleveland, Ohio, June 25, 1971,
704-13.

REFERENCES

1. Goldman, Richard G.; Gurski, Guy S.; and Hawersaat, William H.: Description of SERT II Spacecraft and Mission. NASA TM X-2087, 1970.
2. Stevens, N. John; and Smolak, George R.: Design of the Passive Thermal Control System of the SERT II Satellite. Proceedings of the Symposium on Thermodynamics and Thermophysics of Space Flight. Western Periodicals Co., 1970, pp. 101-120.
3. DePauw, James F.; and Ignaczak, Louis R.: Qualification and Testing of an Electrically Propelled Spacecraft-SERT II. NASA TM X-2199, 1971.
4. Braun, C. E.: A Modified Thermal Analyzer Digital Computer Program for Solution of Heat Transfer Problems. GD/C Program Number 2961. Rep. GD/C-BTD-65-118, General Dynamics/Convair, July 20, 1965.
5. Schultz, H. D.: Thermal Analyzer Computer Program for the Solution of General Heat Transfer Problems. Rep. LR-18902, Lockheed-California Co. (NASA CR-65581), July 16, 1965.
6. Gaski, J. D.; and Lewis, D. R.: IBM-7094-11-DCS Computer Program CO9945, Chrysler Improved Numerical Differencing Analyzer. Rep. TN-AP-66-15, Chrysler Corp. (NASA CR-89100), Apr. 30, 1966.
7. Bevans, J. T.; Ishimoto, T.; Loya, B. R.; and Luedke, E. E.: Prediction of Space Vehicle Thermal Characteristics. TRW Systems Group (AFFDL-TR-65-139, AD-472558), Oct. 1965.
8. Whitehurst, C. A.; and Durbin, W. T.: A Study of the Thermal Conductance of Bolted Joints. Louisiana State Univ. (NASA CR-102639), 1970.
9. Toups, K. A.: A General Computer Program for the Determination of Radiant-Interchange Configuration and Form Factors: CONFAC II. Rep. SID-65-1043-2, North American Aviation (NASA CR-65257), Oct. 1965.

10. Ishimoto, T.; Gaski, J. D.; and Fink, L. C.: Development of Digital Computer Program for Thermal Network Correction. Phase 2: Program Development. Phase 3: Demonstration/Application. TRW-11027-6002-RO-00, TRW Systems (NASA CR-108681), Sept. 1970.

11. Doenecke, Jochen: Adjustment of a Thermal Mathematical Model to Test Data. J. Spacecraft Rockets, vol. 7, no. 6, June 1970, pp. 720-726.

TABLE I. - TIME HISTORY OF COMPONENT POWER DISSIPATIONS

Description	Location	Test time, hr								
		1 to 3	3 to 37	37 to 39	39 to 42	42 to 48	48 to 49	49 to 68	68 to 72	72 to 97
		Heat dissipation, W								
Spacecraft										
B-1 box	Bay 1 upper	1	1	----	-----	----	-----	1	1	1
B-2 box	Bay 1 lower	0.2	0.2	----	-----	----	-----	0.2	0.2	0.2
Power conditioner	Bay 3 side of bay 4	-----	150	----	-----	----	-----	125	125	125
Thruster	Bay 6	-----	90	----	-----	----	-----	90	90	90
Signal conditioner	Bay 7 lower	4.1	4.1	----	-----	----	-----	4	4	4
Spacecraft probe electronics Horizon sensor electronics	Bay 8 upper	12	12	----	-----	----	-----	12	12	12
RFI electronics MESA heater MESA electronics MESA electronics heater	Bay 8 upper	15.4	15.4	----	-----	----	-----	15.4	15.4	15.4
Spacecraft support unit										
Battery	Bay 8	1	1	1.1	1.1	1.1	5.5	5.5	5.5	5.5
CMG	Center bay, rear upper	4.4	4.4	----	4.4	----	4.4	4.4	4.4	4.4
CMG	Center bay, rear lower	4.4	4.4	----	4.4	----	4.4	4.4	4.4	4.4
Tape recorders Two point calibrator Mixers	Bay 2 lower	7.5	7.5	0.5	0.5	0.5	0.5	7.5	7.5	7.5
Main inverter Standby inverter	Bay 4 lower	11.3	11.3	----	11.3	----	11.3	11.3	11.3	11.3
Phase sensitive demodulators Power control electronics unit	Bay 6 lower	6.5	6.5	2.5	4	2.5	4	6.5	6.5	6.5
Transmitters	Bay 8	1.5	1.5	1.5	1.5	1.5	1.5	1.5	1.5	1.5
Time code generator PCM multicoders Subcommutators	Bay 2 upper	24.18	24.18	5.82	5.82	5.82	24.18	24.18	24.18	24.18
Signal conditioner Battery charger Main SMR Standby SMR	Bay 4 upper	10.44	10.44	7.4	7.4	7.4	10.44	10.44	10.44	10.44
Command decoder Command receivers Command relay J-box	Bay 6 upper	0.45	0.45	0.45	0.45	0.45	0.45	0.45	0.45	0.45

TABLE II. - SUMMARY OF CHANGES IN THERMAL CAPACITANCE AND COMPONENT TO STRUCTURE CONDUCTOR VALUES AS A RESULT OF ITERATIVE ANALYSIS

Location of component	*Identity of component*	Thermal capacitance, J/K		Component to structure conductor, W/K	
		Original value	Value from final iteration	Original value	Value from final iteration
		Spacecraft			
Bay 1 upper	B-2 box	5 370	5 370	1.32	1.32
Bay 1 lower	B-1 box	6 820	6 820	↓	↓
Bay 7 upper	B-3 box	4 120	4 120		
Bay 7 lower	*Signal conditioner*	4 310	4 310		
Bay 8 upper	Six beam probe and horizon sensor boxes	13 900	19 000		
Bay 8 lower	Two MESA boxes, B-5 box, and RFI box	12 200	19 000	↓	2.11
Bay 4	*Power conditioner*	6 800	27 100	3.40	7.07
				3.32	5.54
				3.32	5.54
				3.01	3.01
		Spacecraft support unit			
Bay 2 upper	Seven boxes	9 620	9 500	1.32	1.74
Bay 2 lower	Five boxes	9 610	5 700	↓	1.32
Bay 4 upper	Four boxes	10 800	5 700		1.32
Bay 4 lower	Inverters	10 200	5 700		3.16
Bay 6 upper	Three command system boxes	8 700	4 750		1.32
Bay 6 lower	Three boxes	10 200	5 700		2.11
Bay 8 lower	Five boxes	6 420	5 700	↓	1.32
Bay 8	Battery	16 200	7 600	1.39	1.32
Center bay	CMG (typical)	6 910	1 900	.132	.527

TABLE III. - TEMPERATURE COMPARISONS

(a) Spacecraft

Temperature location	Prediction compared to thermocouple		Thermocouple compared to thermistor steady-state extremes, °C	Figures
	Transient slope	Steady-state extremes, °C		
Structure				
Skins				
Bay 1	----	(a)	-2/-3	7
Bay 2	Good	+1/-3	(b)	8
Bay 4	Good	+4/-4	-3/-4	9 to 11
Bay 7	----	(a)	-2/-3	12
Bay 8	----	(a)	+2/+1	13
Bulkheads				
Bay 1 to 2	Good	+1/0	+2/+1	14
Bay 2	↓	+2/+1	(b)	15
Bay 2 to 3		+1/0	↓	16
Bay 3 to 4	↓	-2/-5		17
Bay 4	Fair	-1/-3		18
Bay 4 to 5	Good	0/-1		19
Bay 6	↓	0/0	↓	20
Bay 6 to 7		+2/+2	-2/-3	21
Bay 8	↓	-1/-1	(b)	22
Trays				
Bay 8 upper	Good	0/0	+1/-1	23
Bay 8 lower	Good	-2/-3	-2/-3	24
Thruster interface	Good	-1/-2	0/-1	25
Structure average	Good	0/-1	-1/-2	--
Components				
Power conditioner baseplate	Good	[c] +4/+3	(b)	26
Thruster arc chamber	Poor	+5/-5	+100	27
BACS bottle	Good	[c] 0/-2	(b)	28
Beam probe electronics	↓	+7/+6	↓	23
Space probe electronics		+3/+2		↓
1 G-2 horizon sensor electronics		+3/+3		
Converter	↓	+3/+2		↓
MESA	Fair	-2/-3		24
MESA electronics	Fair	-3/-3		↓
RFI electronics	Good	-1/-1		
B-5 box	Good	-2/-2	↓	↓
Component average	Good	[d] +1/0	(b, d)	--

[a] Set equal.
[b] Not available.
[c] Thermistor.
[d] Except thruster.

TABLE III. - Concluded. TEMPERATURE COMPARISONS

(b) Spacecraft support unit

Temperature location	Prediction compared to thermocouple		Thermocouple compared to thermistor steady-state extremes, ^{o}C	Figures
	Transient slope	Steady-state extremes, ^{o}C		
		Structure		
Skins				
Bay 1	(a)	(a)	-3/-4	29
Bay 2	Good	-1/-2	-3/-4	30
Bay 3	↓	+1/-1	-3/-4	31
Bay 4		+3/-3	-1/-4	32
Bay 5		+1/-1	-2/-3	33
Bay 6		-3/-4	-3/-4	34
Bay 7	(a)	(a)	-3/-4	35
Bay 8	(a)	(a)	-2/-3	36
Bulkheads				
Bay 2	Good	-3/-4	-1/-2	37
Bay 4	↓	-3/-4	0/-2	38
Bay 6		-3/-4	0/-2	39
Bay 8		0/-2	-1/-2	40
Trays				
Bay 2 upper	Good	-2/-3	(b)	41
Bay 2 lower	Good	-1/-2	↓	42
Bay 4 upper	Fair	+1/-2		43
Bay 4 lower	Good	-2/-3		44
Bay 6 upper	↓	-2/-3		45
Bay 6 lower		-1/-2		46
Bay 8		-3/-4		47
CMG shelf		+1/-1		48
Structure average	Good	-1/-3	-2/-3	--
		Components		
Battery	Good	+2/-2	0/-2	49
CMG's	↓	+1/-2	(b)	50 to 53
Tape recorders		0/-2	+2/+1	42
Transmitters		+1/-1	0/-2	47
Inverters		+1/-4	+3/-1	44
Bay 2 upper		+10/0	(b)	41
Bay 2 lower		+6/-2	↓	42
Bay 4 upper		+6/0		43
Bay 4 lower		+2/-3		44
Bay 6 upper		0/-4		45
Bay 6 lower		0/-2		46
Bay 8	↓	+2/-2	↓	47
Component average	Good	+3/-2	+1/-1	--

[a]Set equal.

[b]Not available.

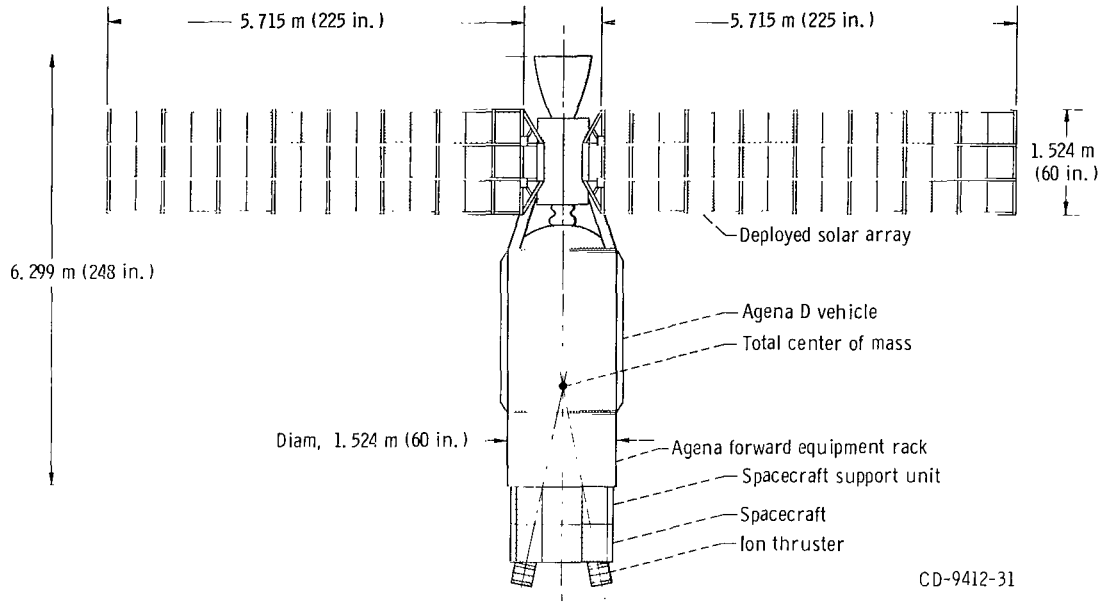

Figure 1. - SERT II satellite.

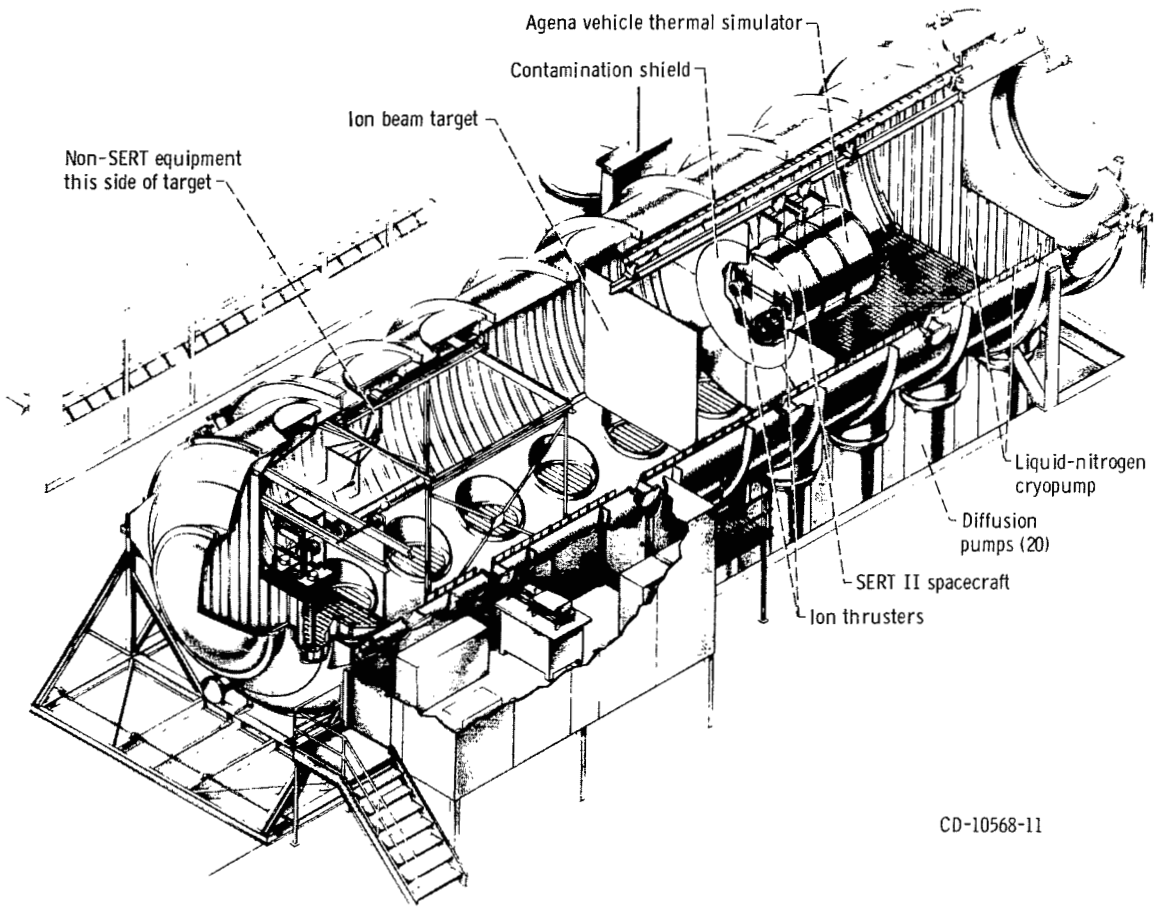

(a) General layout of facility.

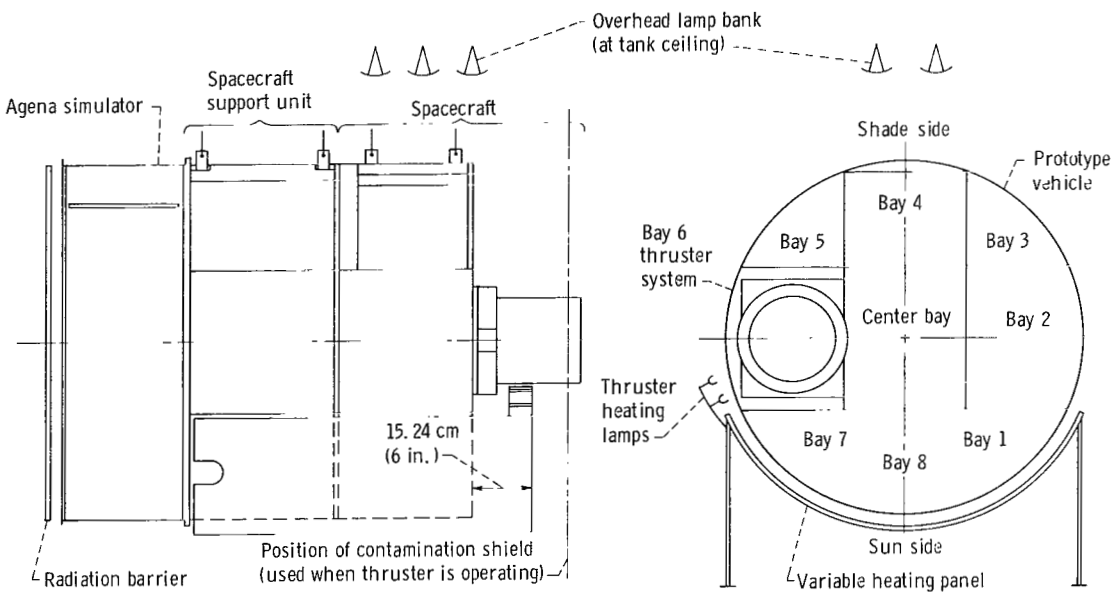

(b) Arrangement of heating devices.

Figure 2. - SERT II in thermal vacuum test facility.

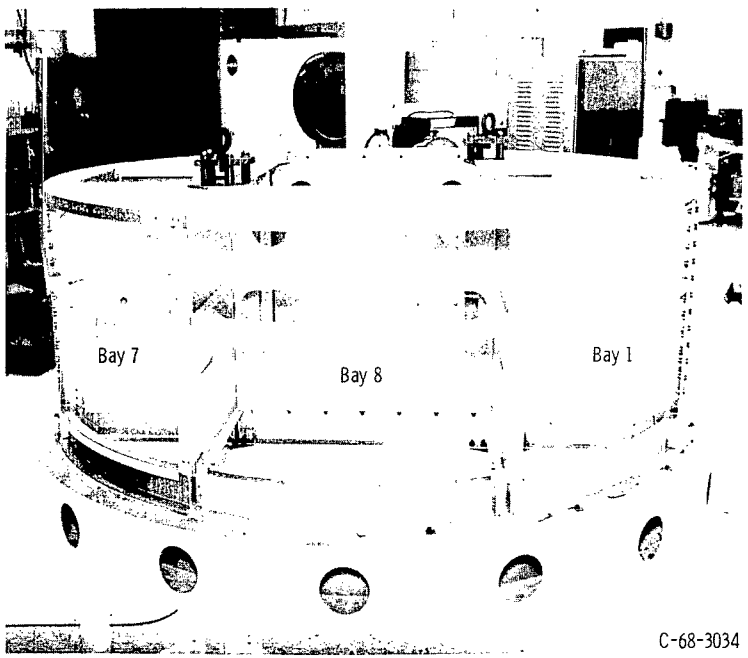

(a) Spacecraft bay 1, 7 and 8 structure details (trays and components removed).

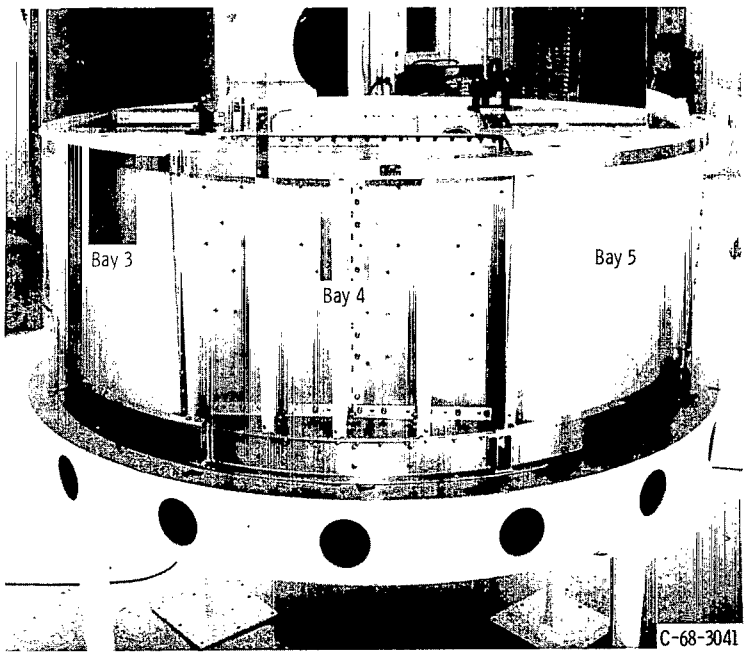

(b) Spacecraft bay 3, 4, and 5 structure details (trays and components removed).

Figure 3. - Structure and component details.

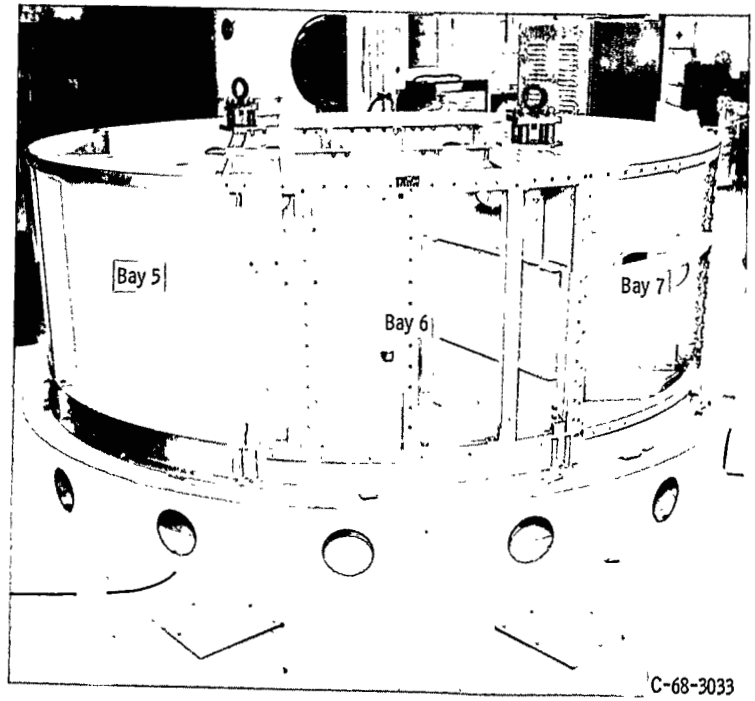

(c) Spacecraft bay 5, 6, and 7 structure details (trays and components removed).

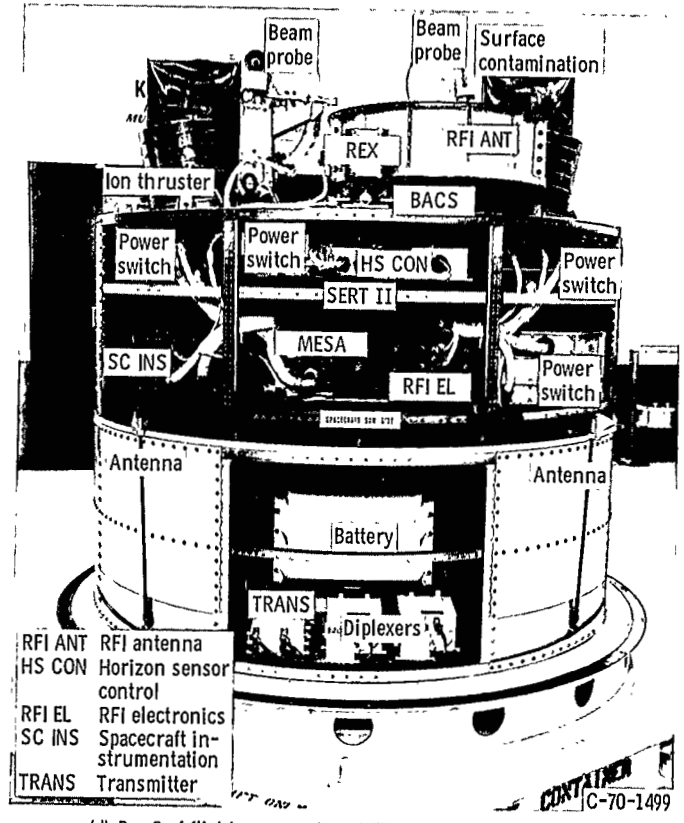

(d) Bay 8 of flight spacecraft and flight spacecraft support unit.

Figure 3. - Continued.

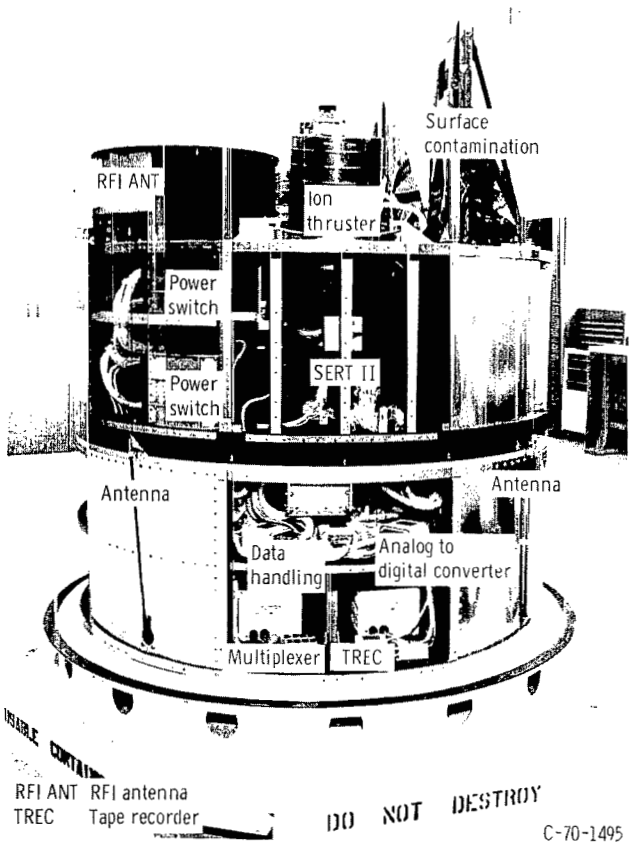

(e) Bay 2 of flight spacecraft and flight spacecraft support unit.

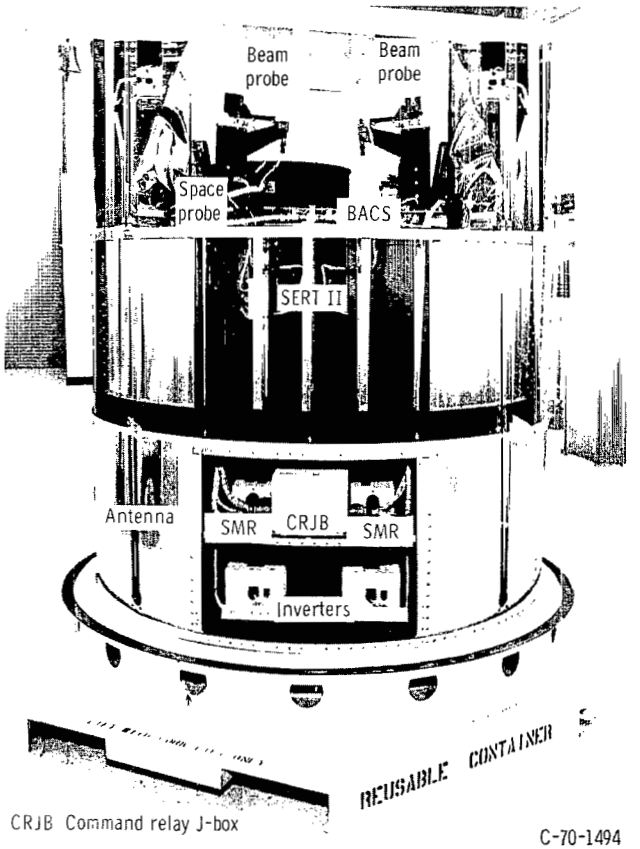

(f) Bay 4 of flight spacecraft and flight spacecraft support unit.

Figure 3. - Concluded.

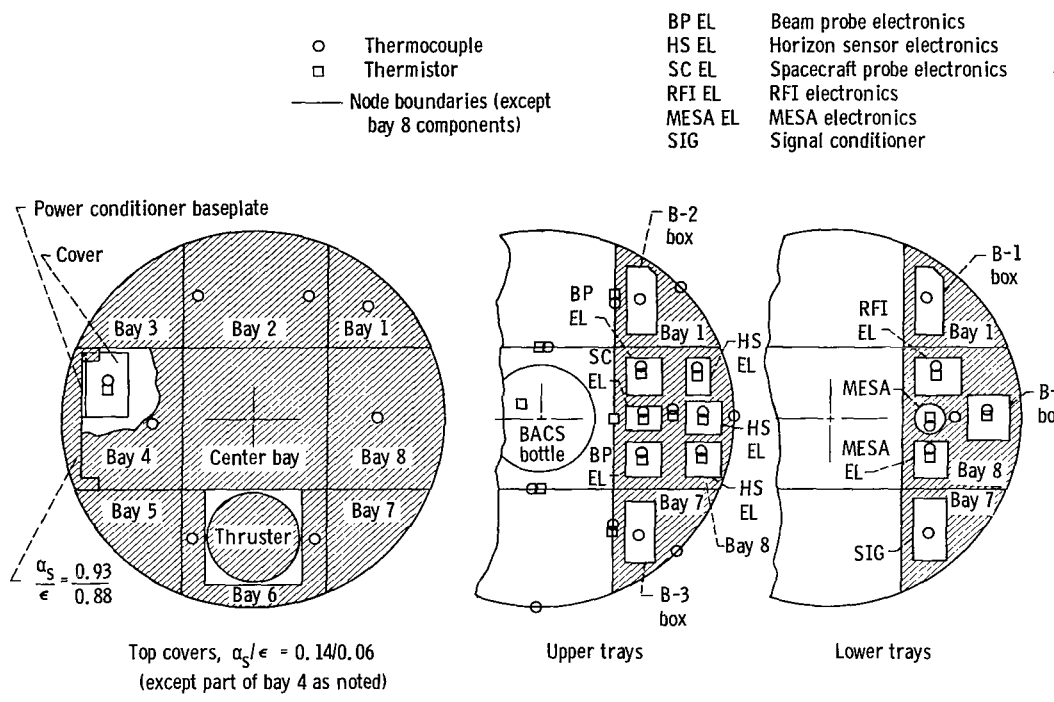

(a) Top views.

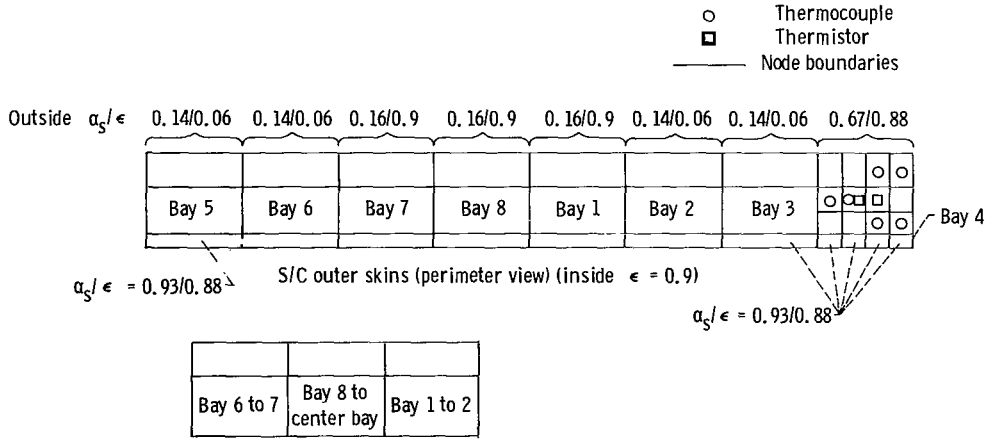

Typical S/C internal bulkhead (ϵ = 0.9)

(b) Outer skins and bulkheads.

Figure 4. - Spacecraft details and instrumentation.

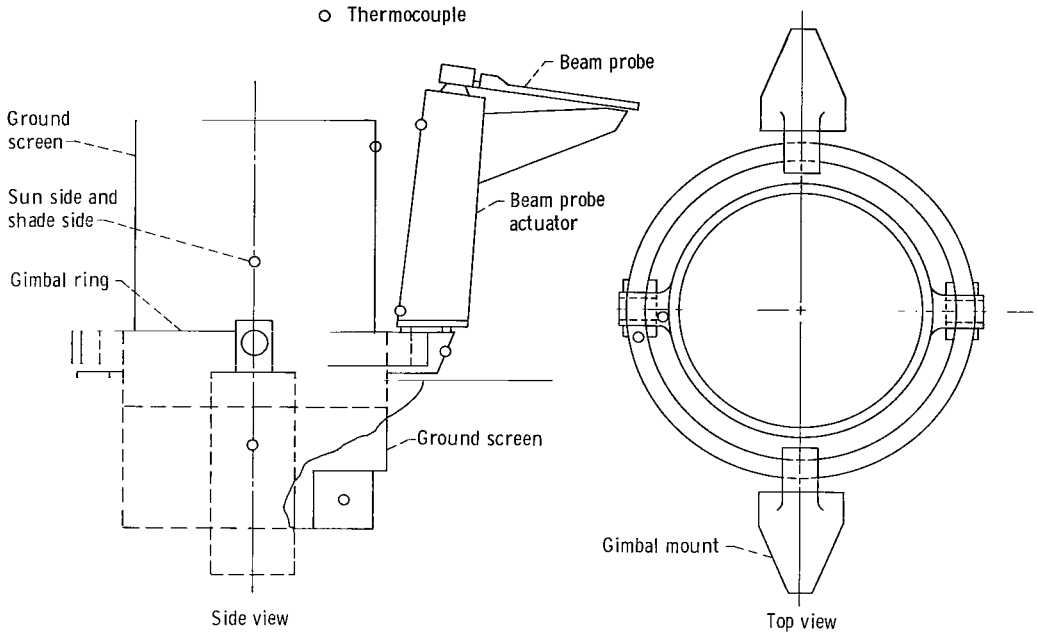

(c) Thruster.

Figure 4. - Concluded.

TCG	Time code generator
SUB	Subcommutator
MULT	Multicoder
SIG	Signal conditioner
BAT CH	Battery charger
PR CMG	Prototype CMG
CMG SIM	CMG simulator
BAT	Battery
CRJB	Command relay J-box
COMD	Command decoder
COMR	Command receiver
CAL	Calibrator
MIX	Mixer
TREC	Tape recorder
INV	Inverter
EX CMG	Experimental CMG
CMG SIM	CMG simulator
TR	Transmitter
DIP	Diplexer
HYB	Hybrid
DEM	Phase sensitive demodulator
PC EU	Power control electronics unit

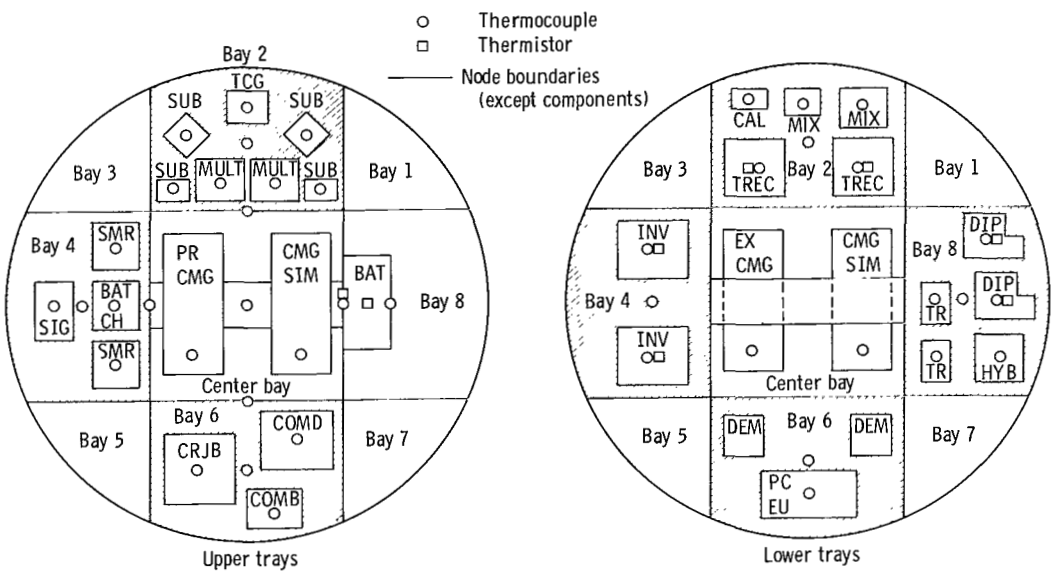

(a) Top views.

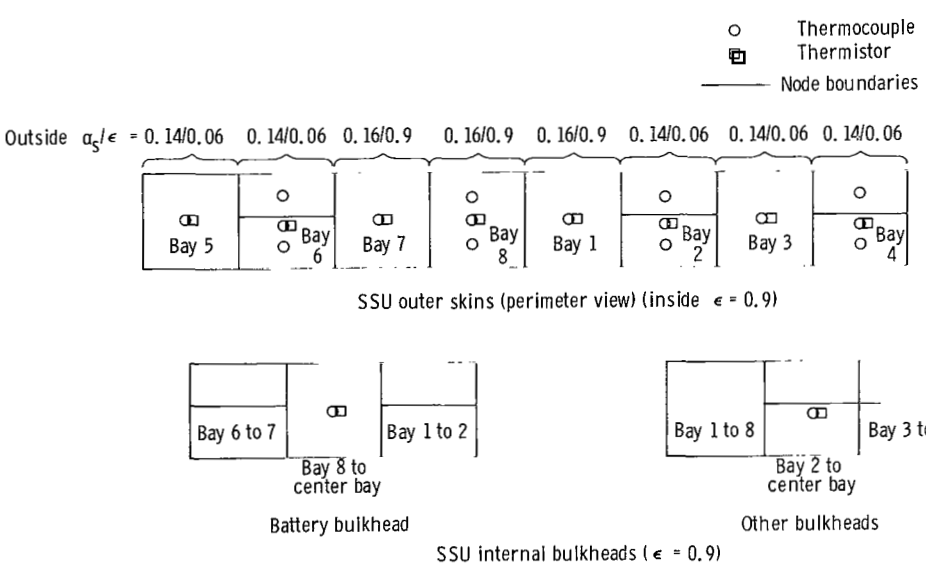

(b) Outer skins and bulkheads.

Figure 5. - Spacecraft support unit details and instrumentation.

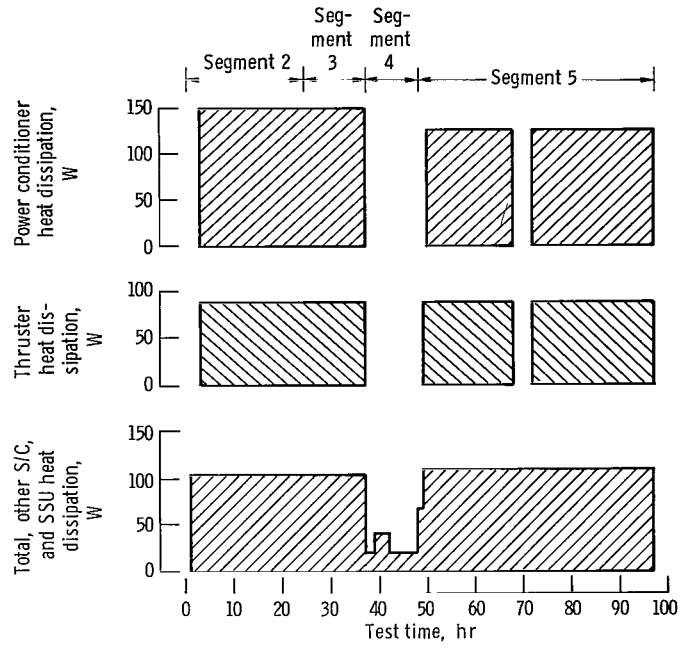

Figure 6. - Heat dissipation plotted against time.

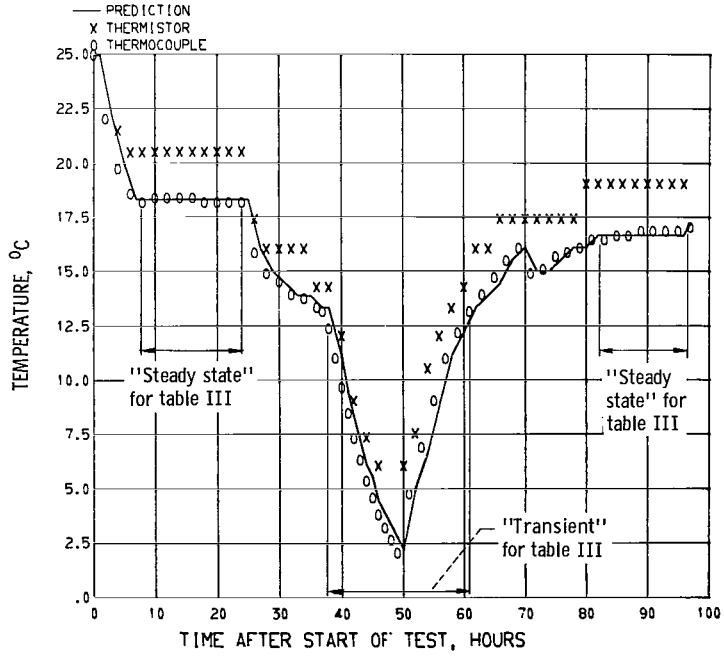

Figure 7. - Spacecraft bay 1 skin.

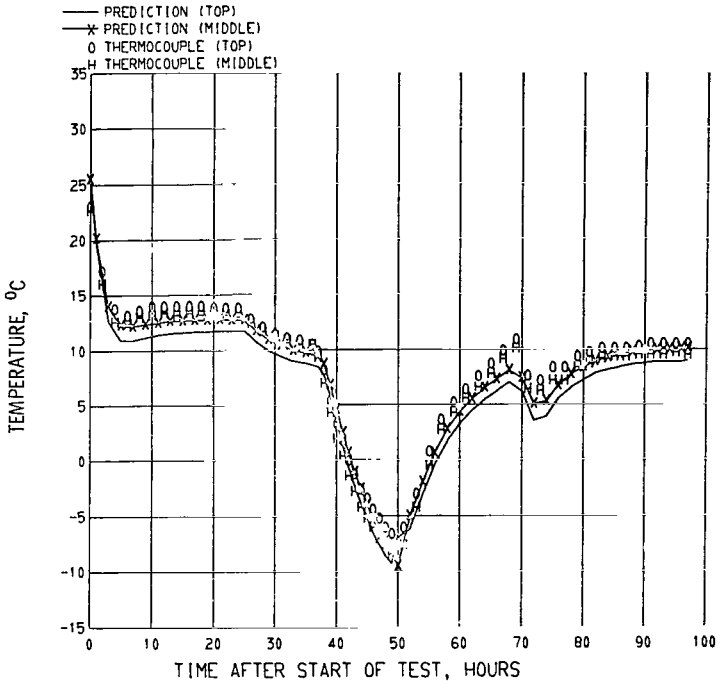

Figure 8. - Spacecraft bay 2 skin.

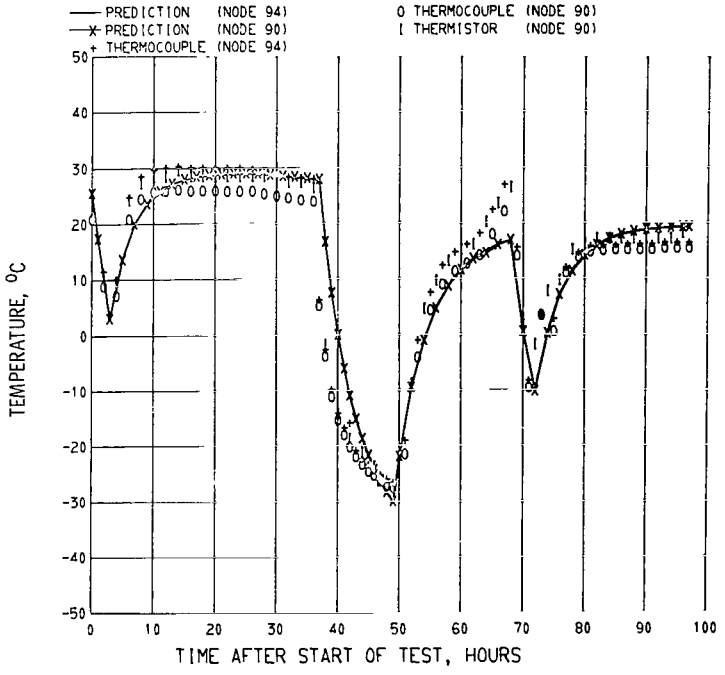

Figure 9. - Spacecraft bay 4 radiator middle area.

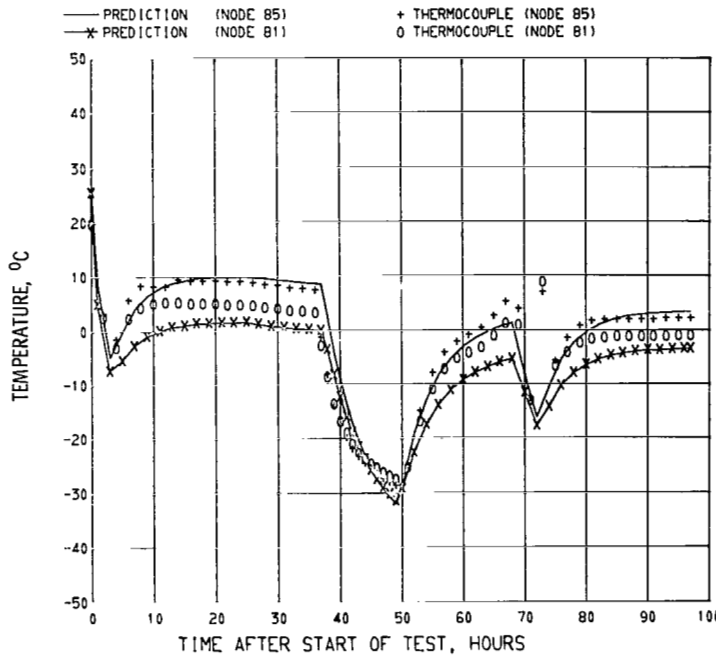

Figure 10. - Spacecraft bay 4 radiator top area.

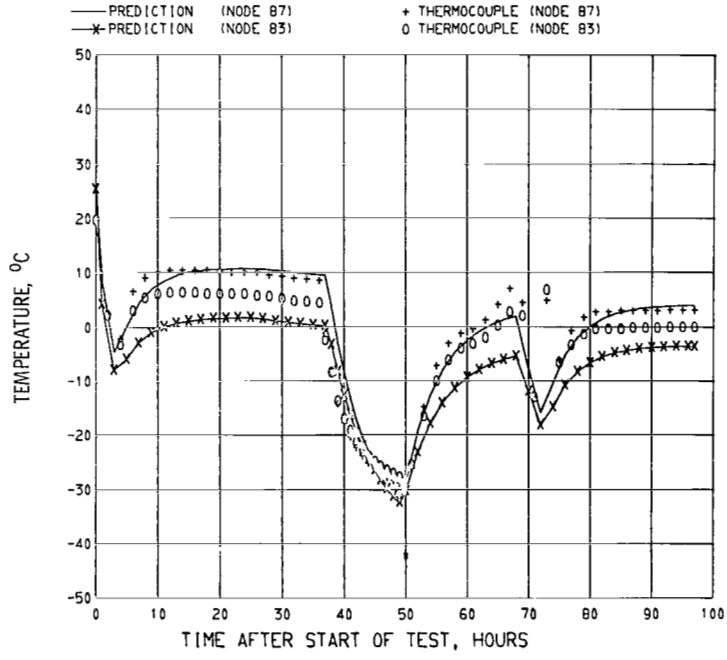

Figure 11. - Spacecraft bay 4 radiator bottom area.

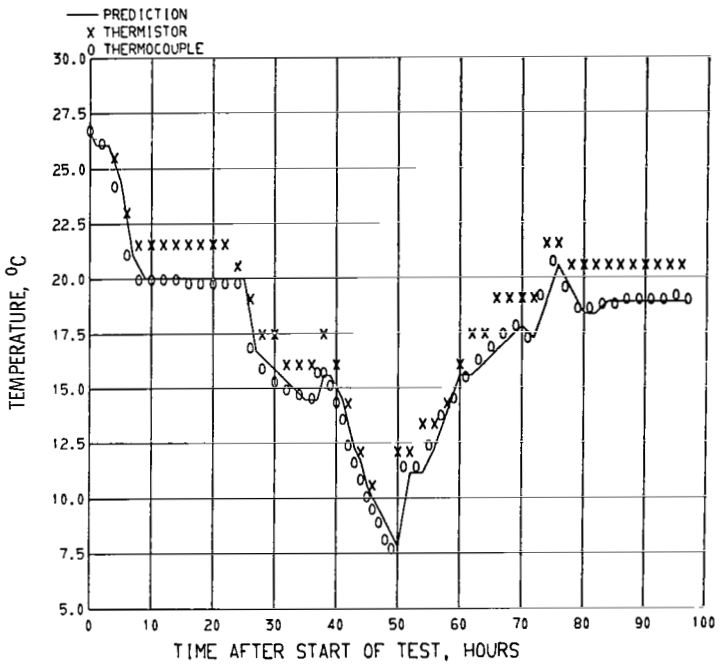

Figure 12. - Spacecraft bay 7 skin.

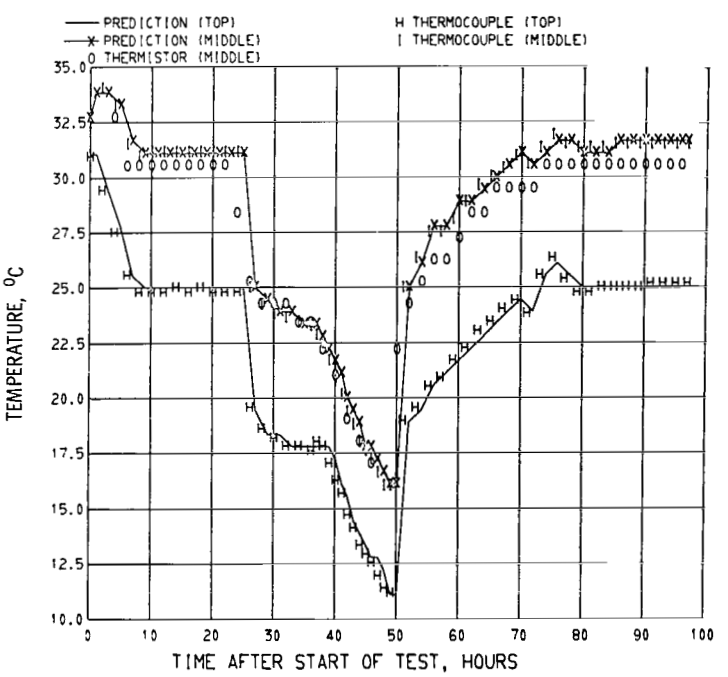

Figure 13. - Spacecraft bay 8 skin.

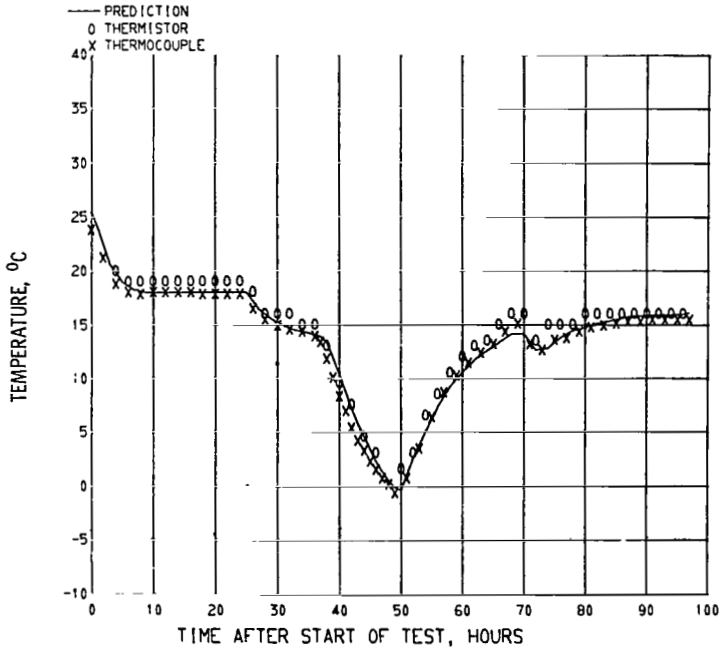

Figure 14. - Spacecraft bay 1 to 2 bulkhead.

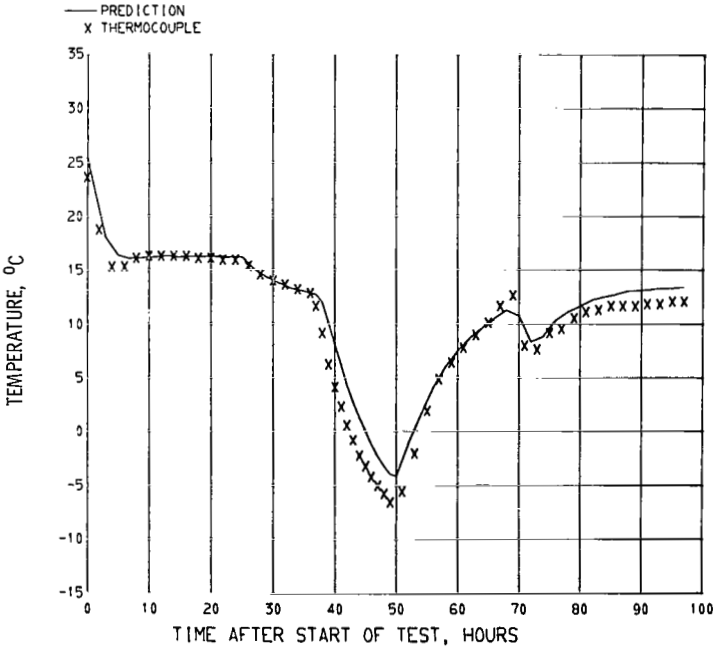

Figure 15. - Spacecraft bay 2 bulkhead.

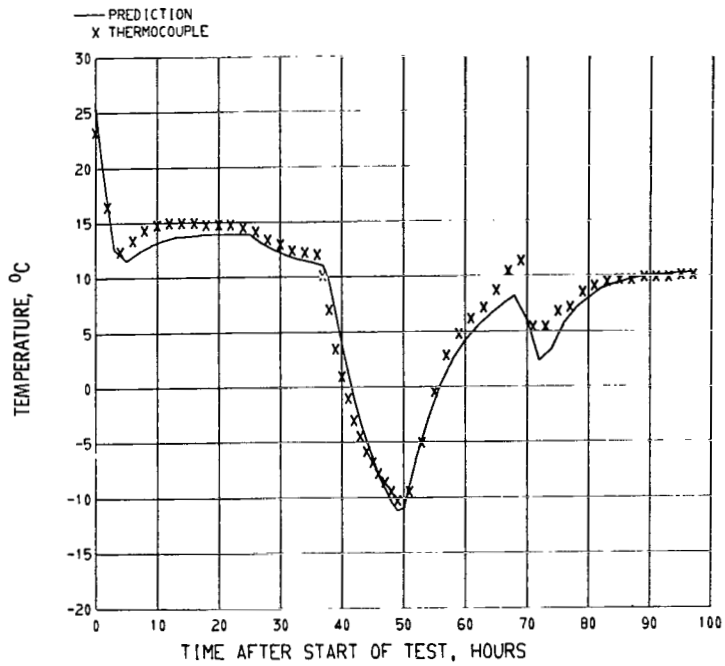

Figure 16. - Spacecraft bay 2 to 3 bulkhead.

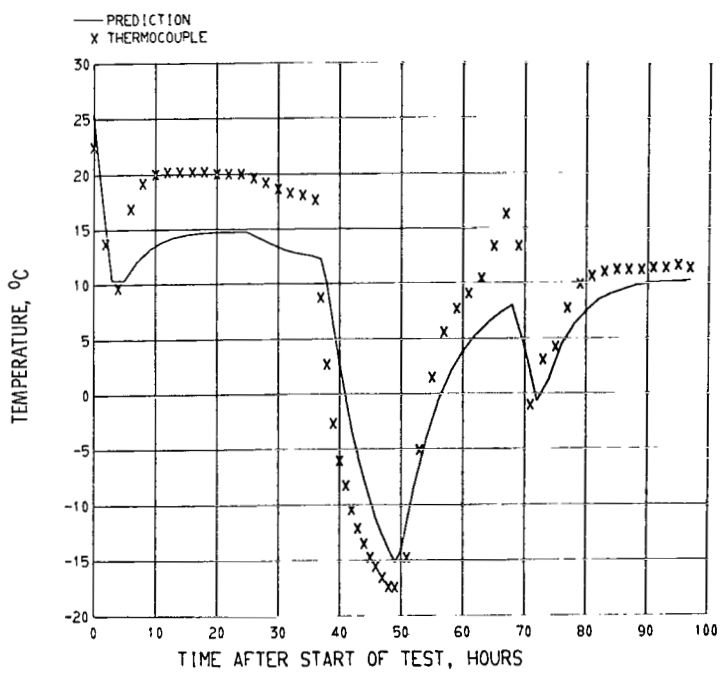

Figure 17. - Spacecraft bay 3 to 4 bulkhead.

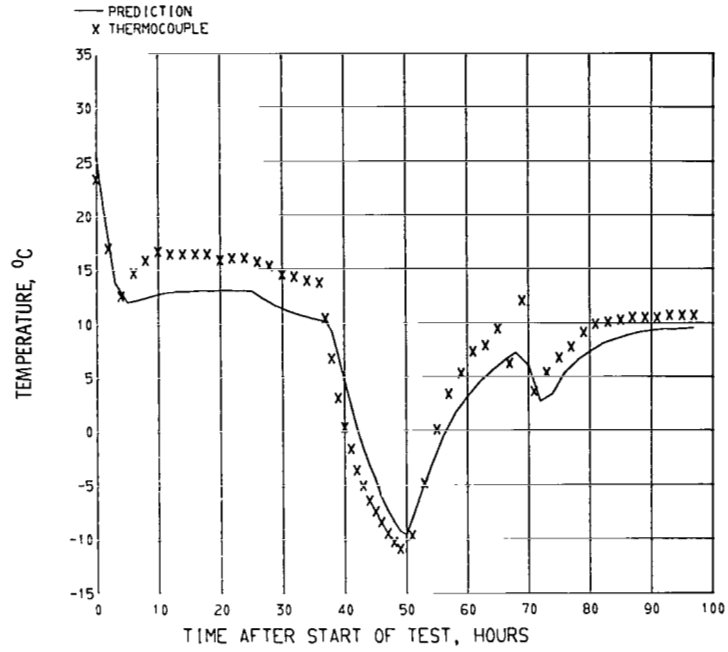

Figure 18. - Spacecraft bay 4 bulkhead.

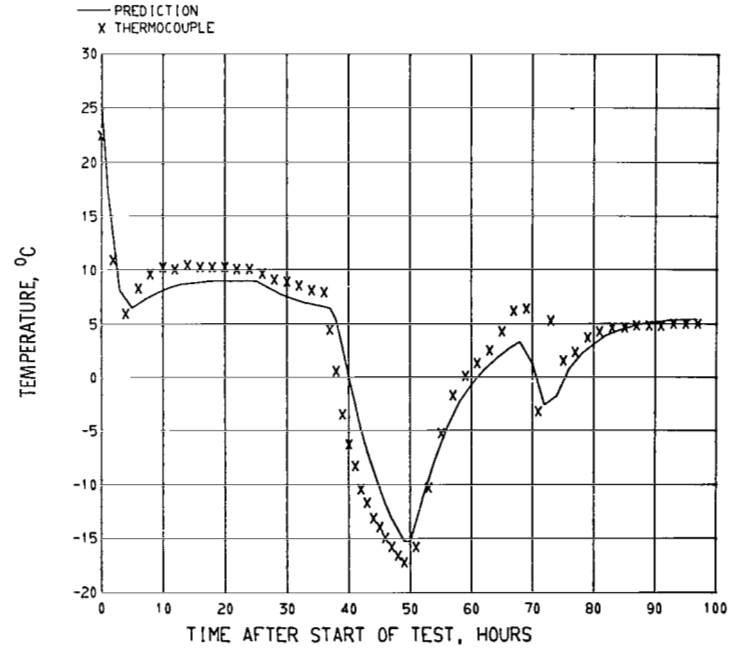

Figure 19. - Spacecraft bay 4 to 5 bulkhead.

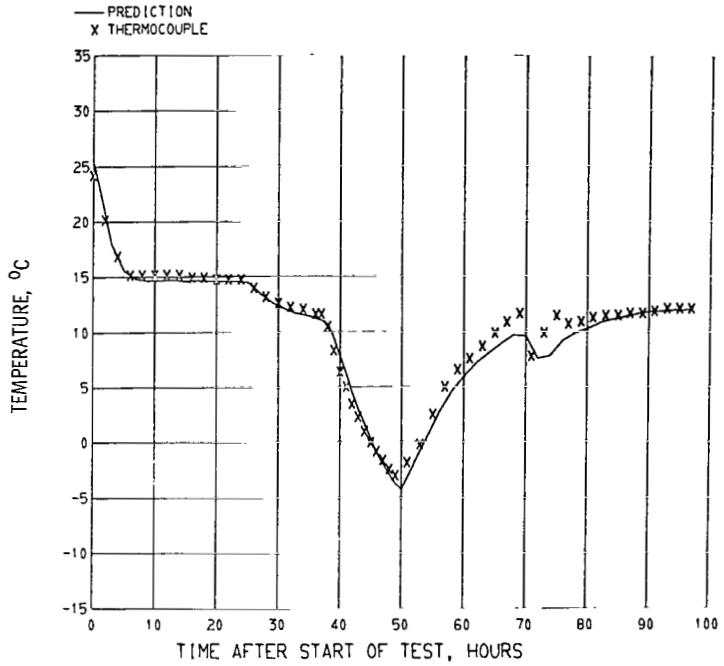

Figure 20. - Spacecraft bay 6 bulkhead.

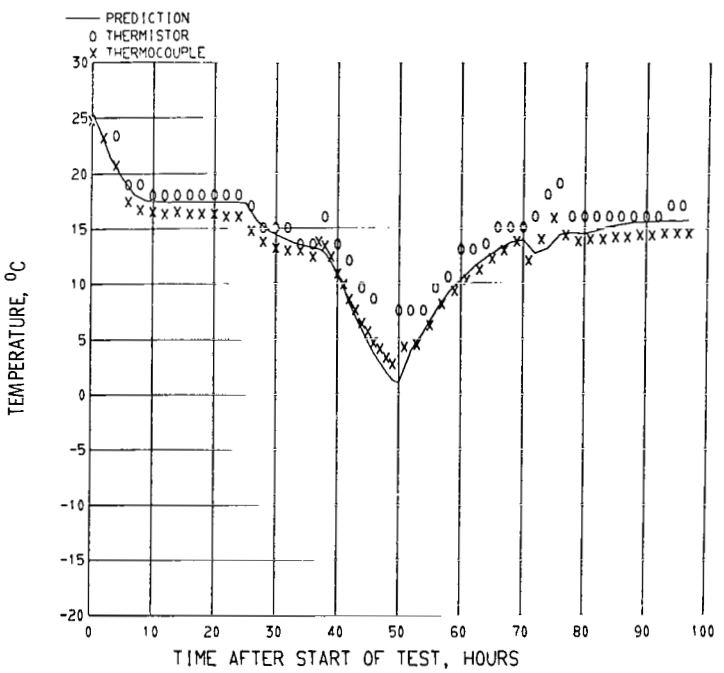

Figure 21. - Spacecraft bay 6 to 7 bulkhead.

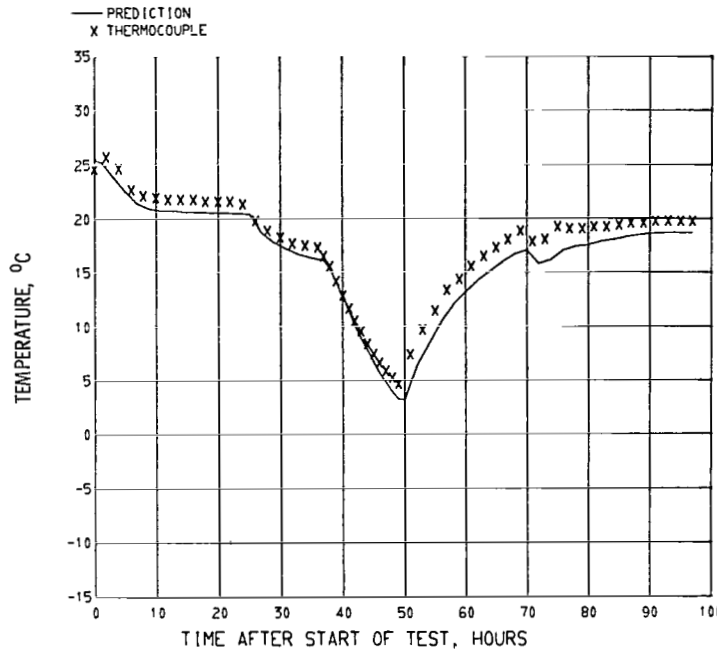

Figure 22. - Spacecraft bay 8 bulkhead.

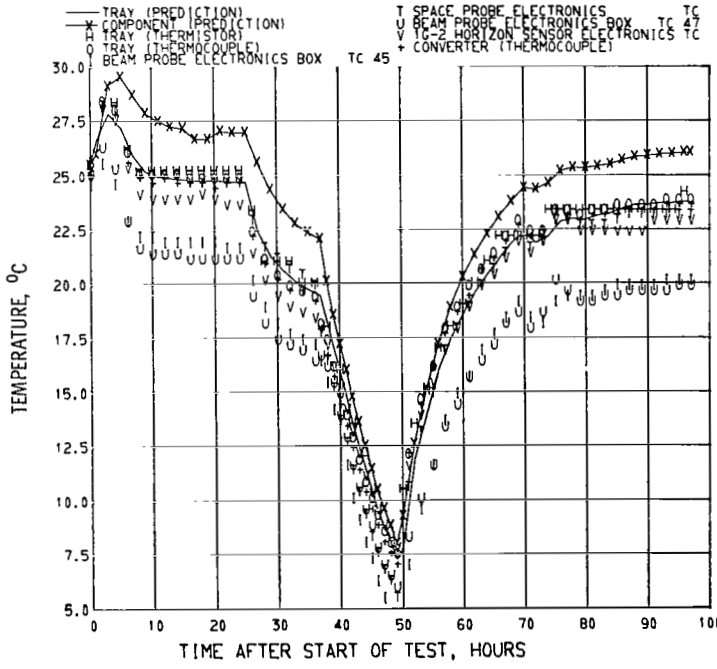

Figure 23. - Spacecraft bay 8 upper tray.

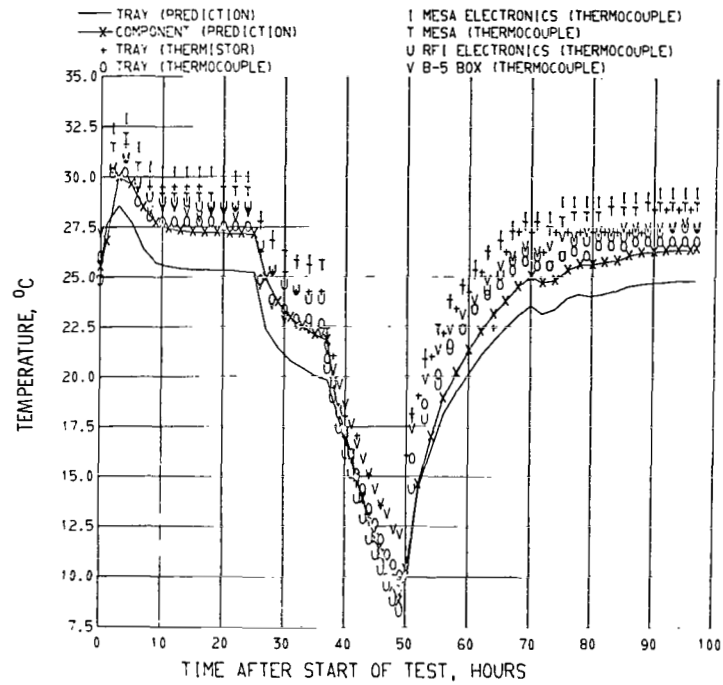

Figure 24. - Spacecraft bay 8 lower tray.

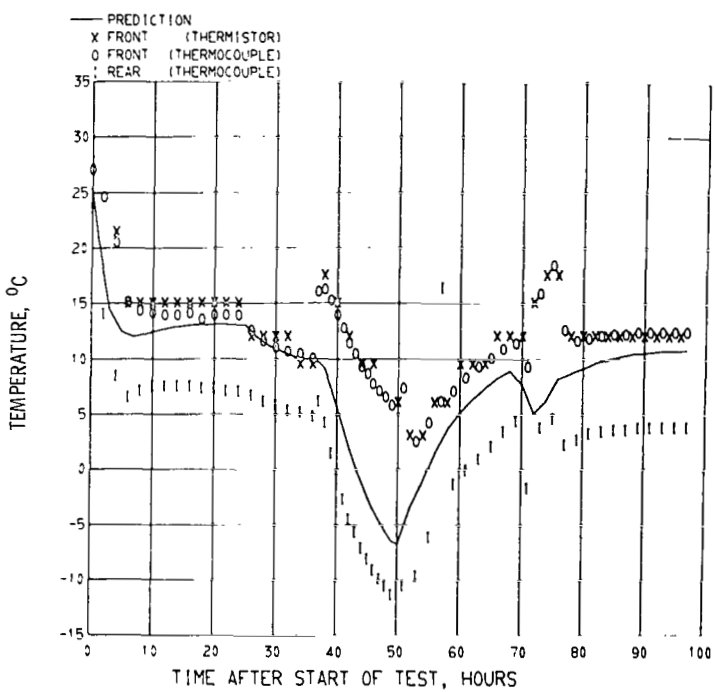

Figure 25. - Spacecraft thruster interface.

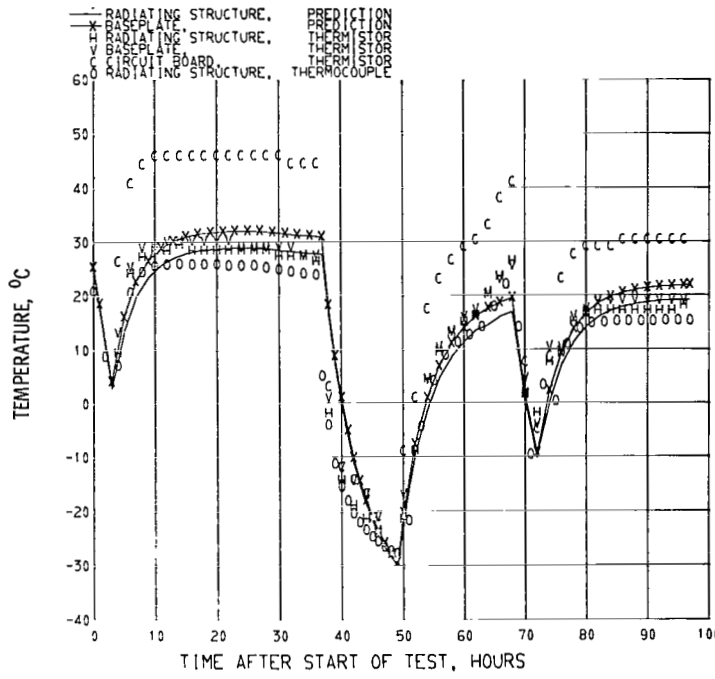

Figure 26. - Spacecraft power conditioner.

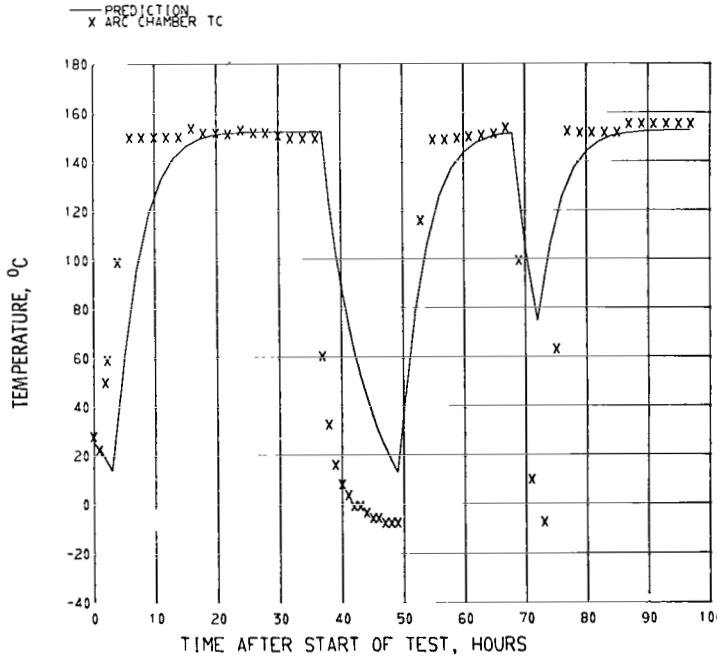

Figure 27. - Spacecraft thruster.

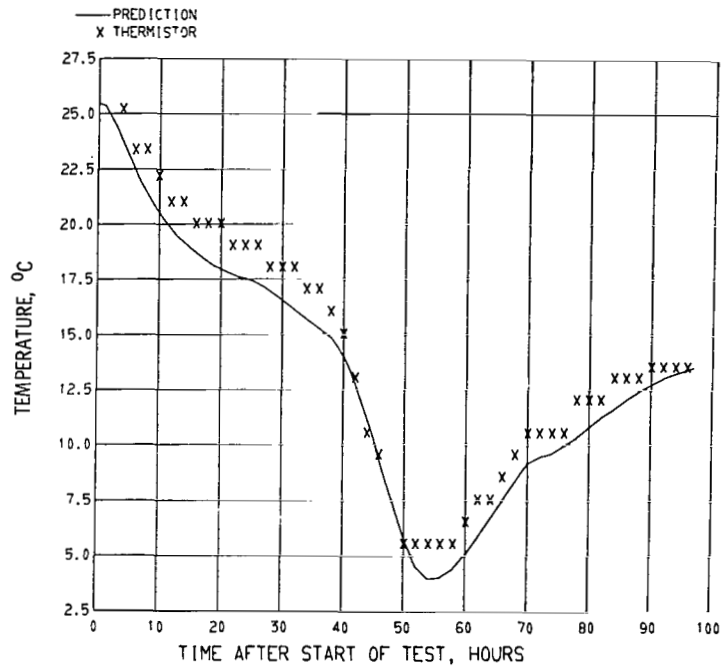

Figure 28. - Spacecraft backup acquisition system bottle.

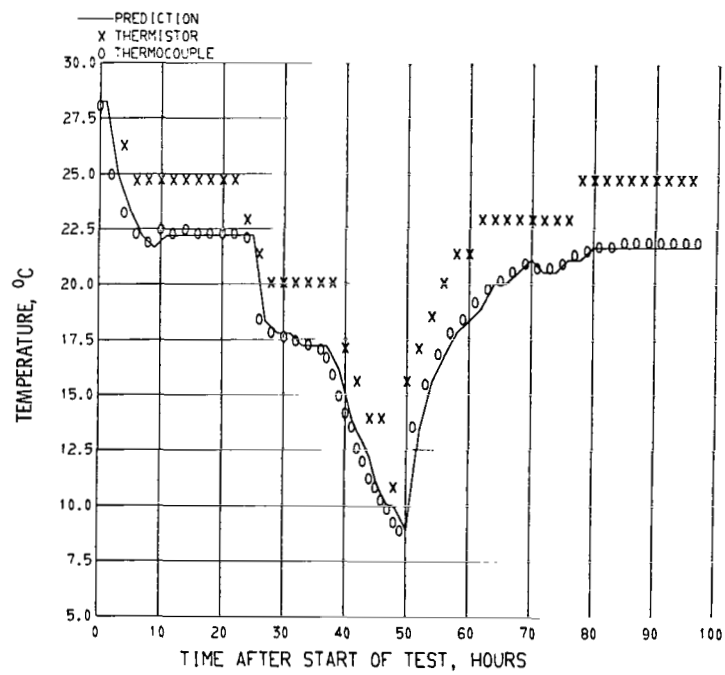

Figure 29. - Spacecraft support unit bay 1 skin.

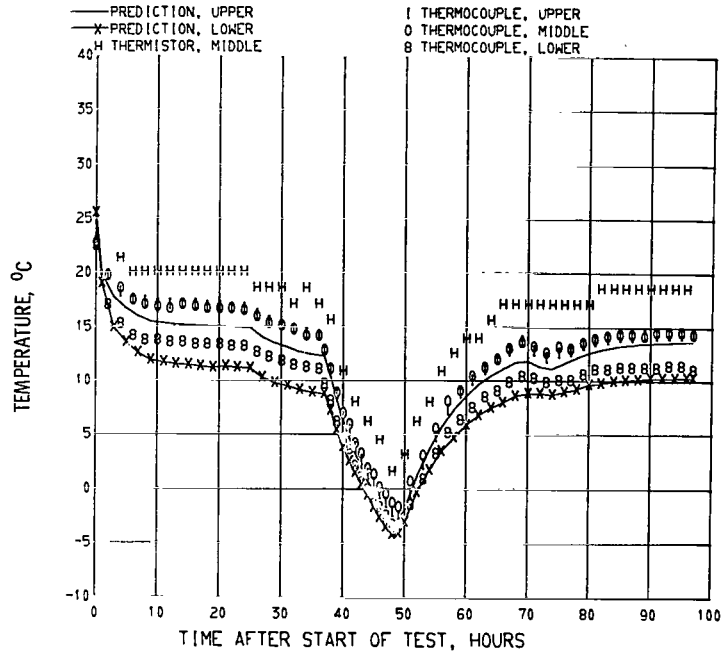

Figure 30. - Spacecraft support unit bay 2 skin.

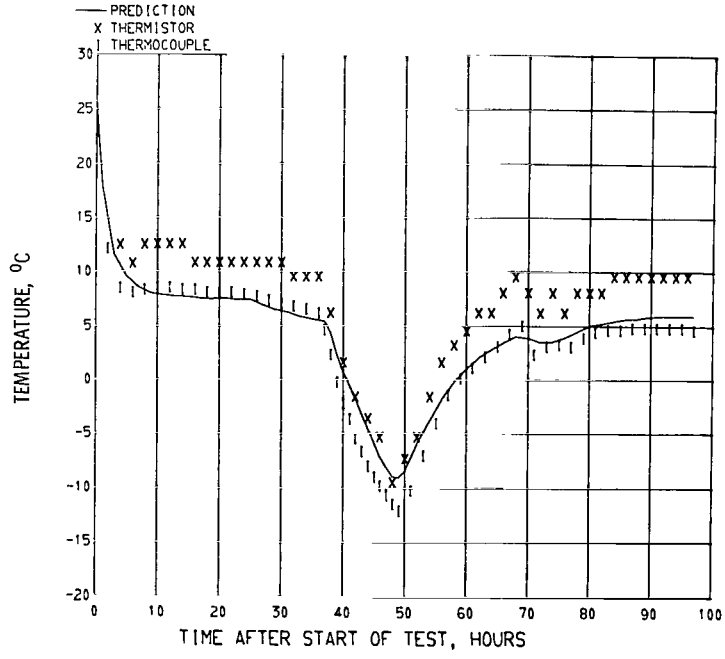

Figure 31. - Spacecraft support unit bay 3 skin.

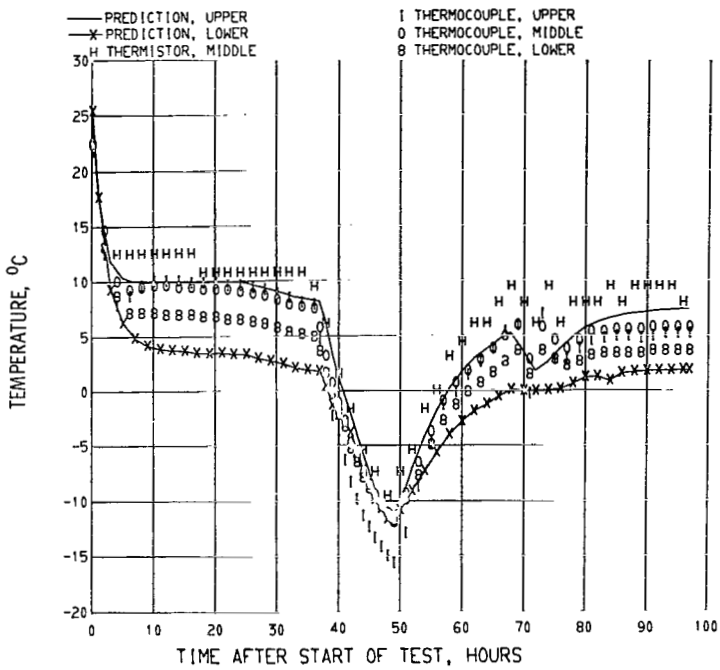

Figure 32. - Spacecraft support unit bay 4 skin.

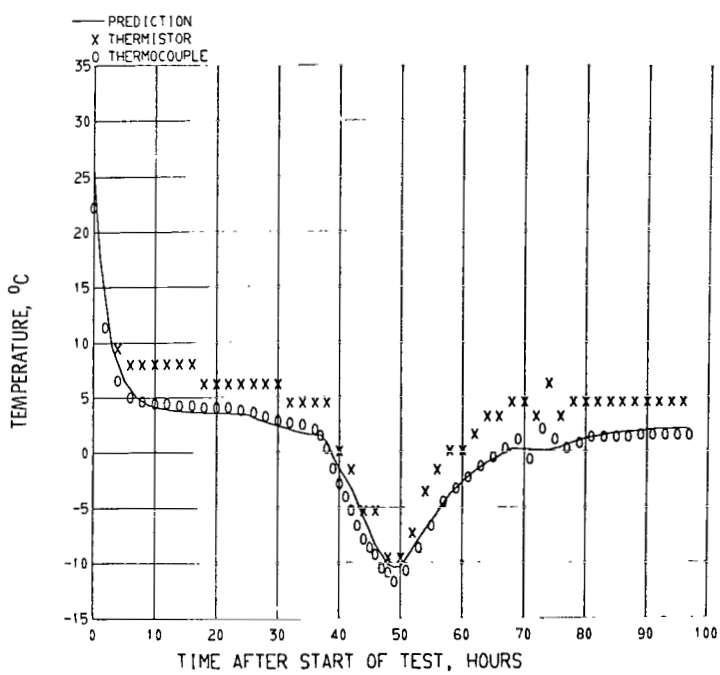

Figure 33. - Spacecraft support unit bay 5 skin.

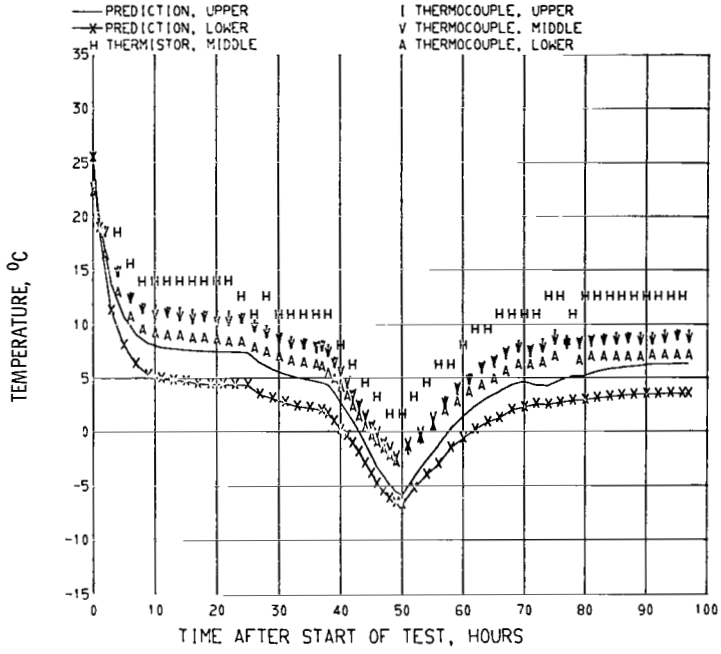

Figure 34. - Spacecraft support unit bay 6 skin.

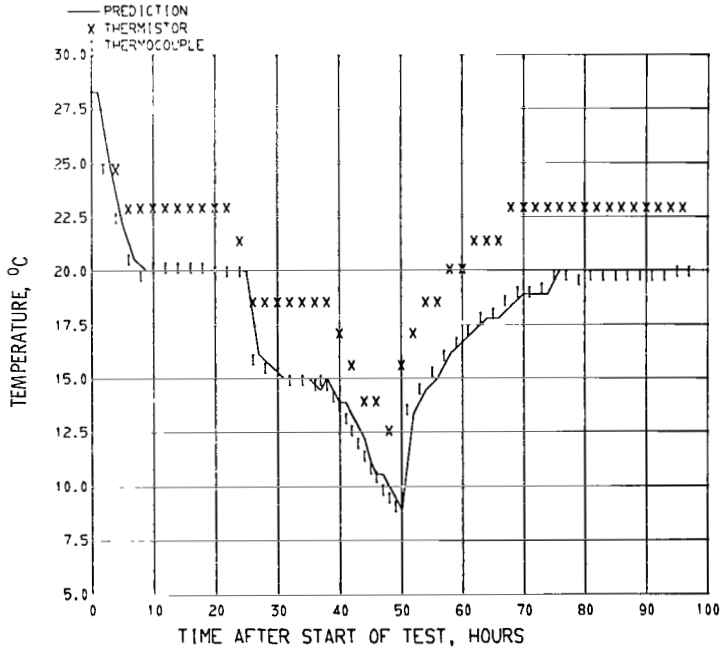

Figure 35. - Spacecraft support unit bay 7 skin.

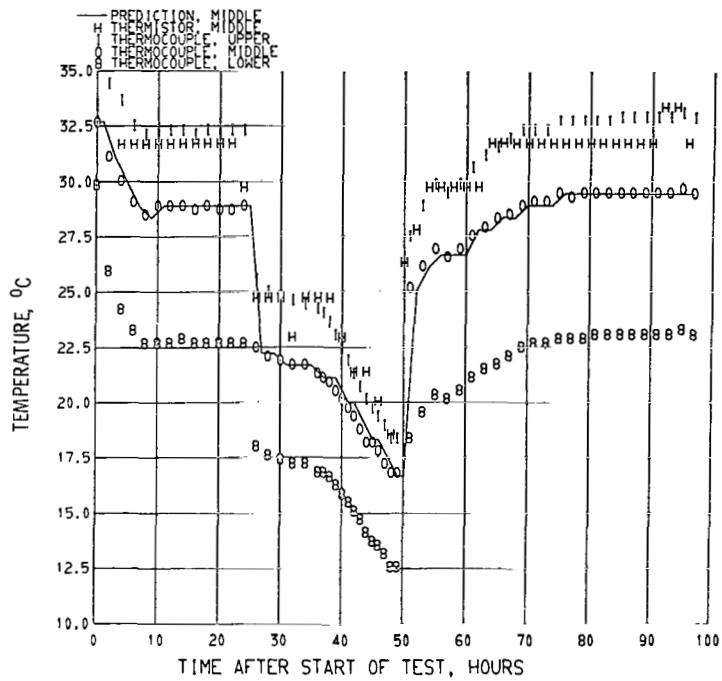

Figure 36. - Spacecraft support unit bay 8 skin.

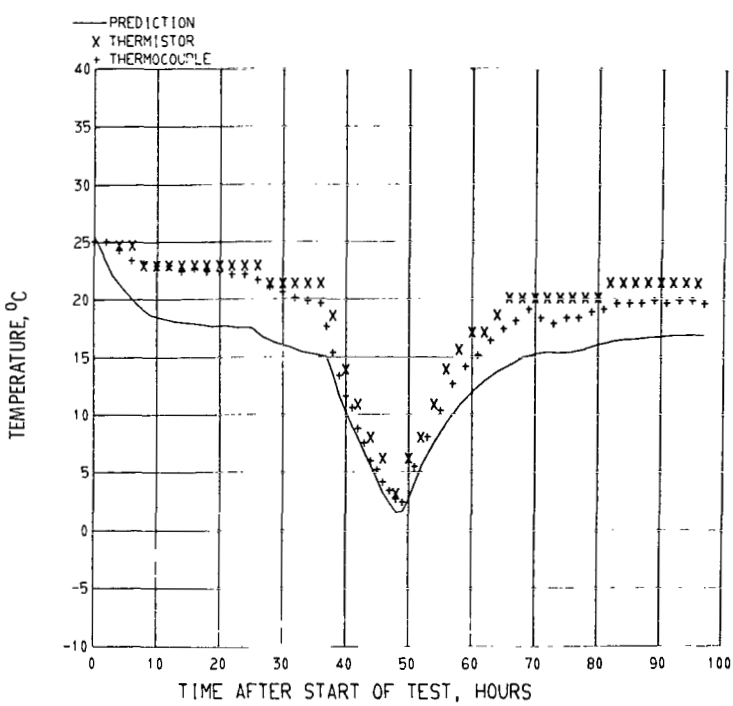

Figure 37. - Spacecraft support unit bay 2 bulkhead.

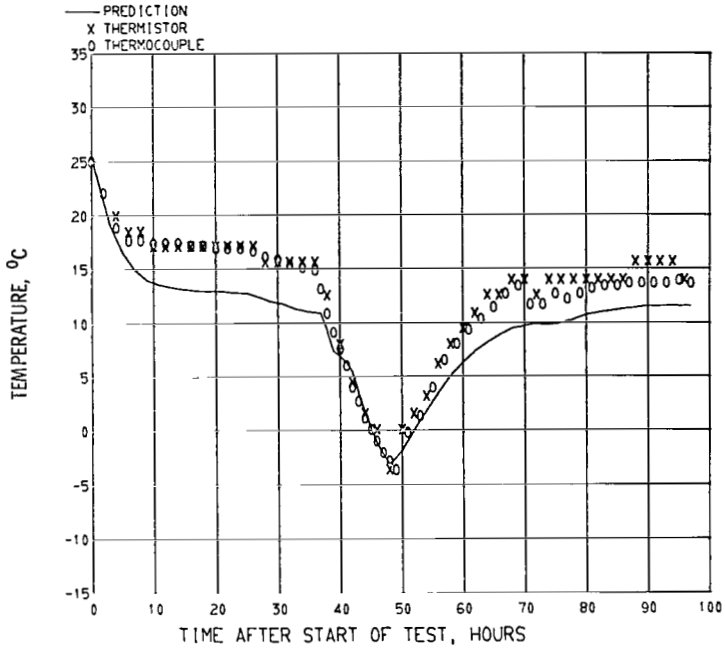

Figure 38. - Spacecraft support unit bay 4 bulkhead.

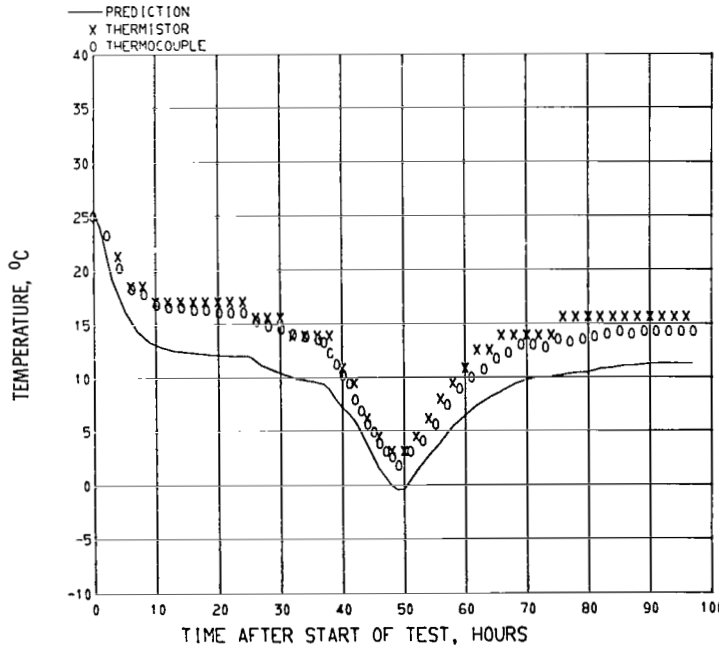

Figure 39. - Spacecraft support unit bay 6 bulkhead.

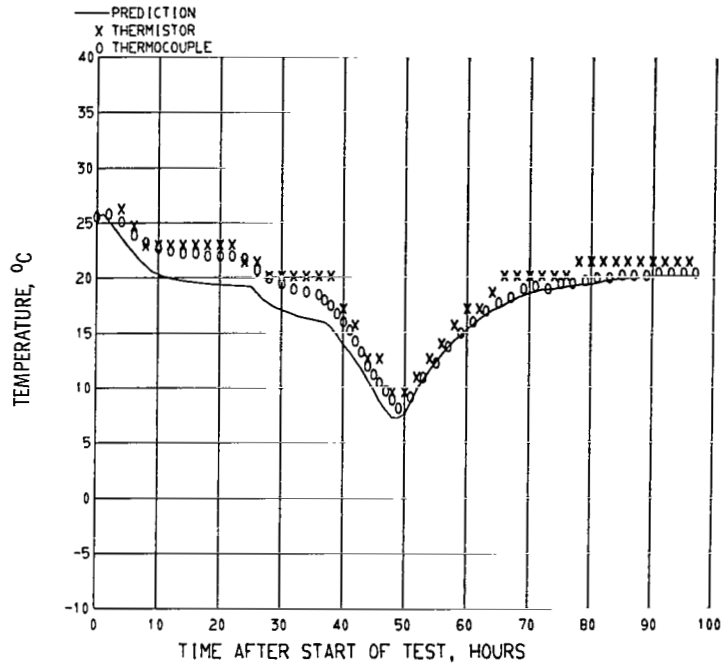

Figure 40. - Spacecraft support unit bay 8 bulkhead.

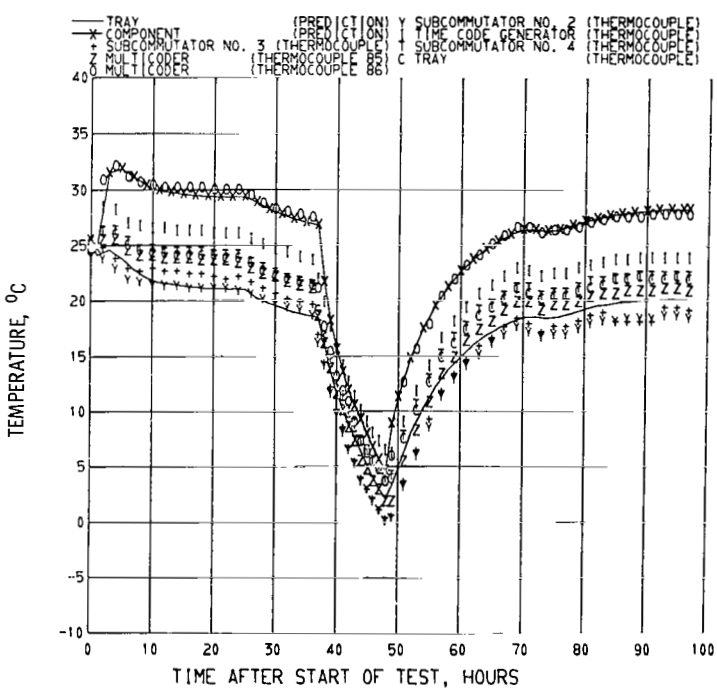

Figure 41. - Spacecraft support unit bay 2 upper area.

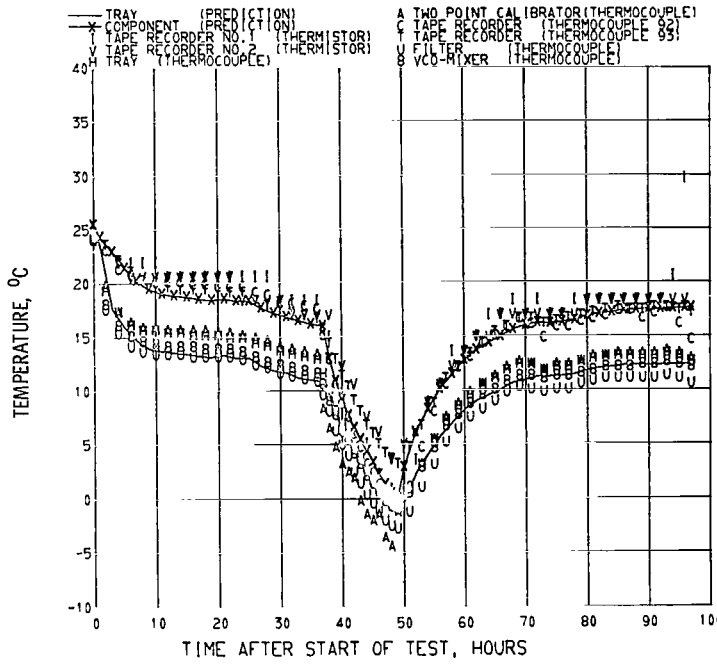

Figure 42. - Spacecraft support unit bay 2 lower area.

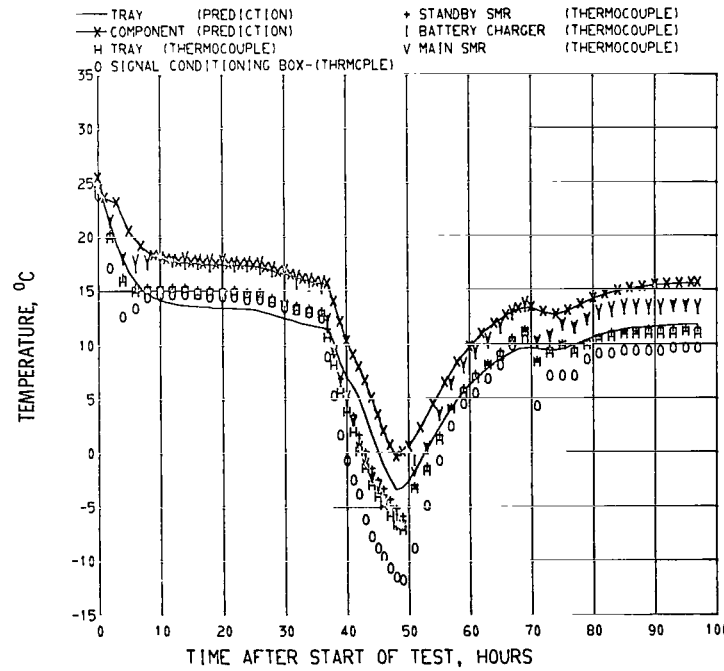

Figure 43. - Spacecraft support unit bay 4 upper area.

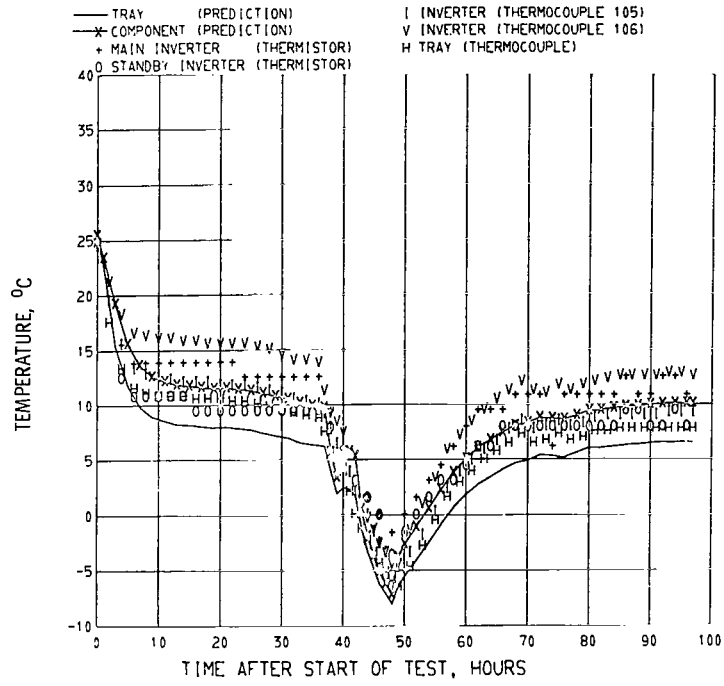

Figure 44. - Spacecraft support unit bay 4 lower area.

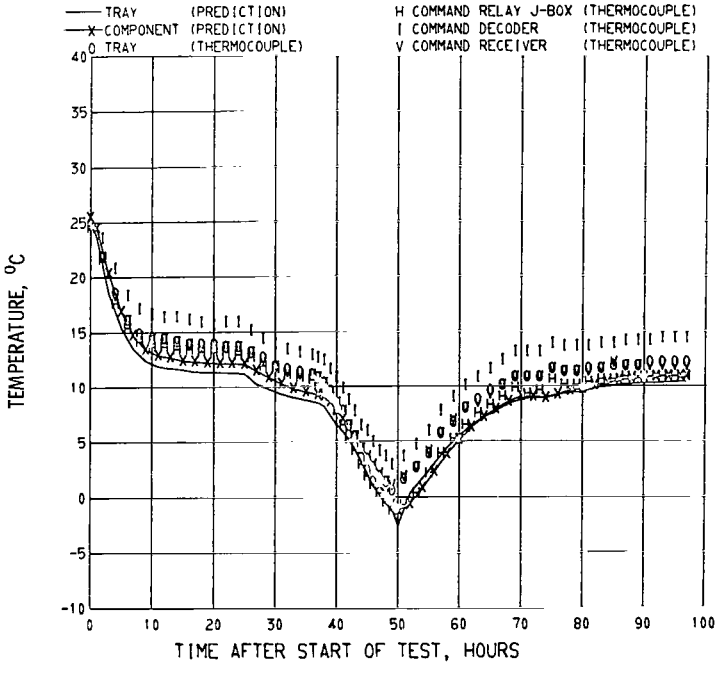

Figure 45. - Spacecraft support unit bay 6 upper area.

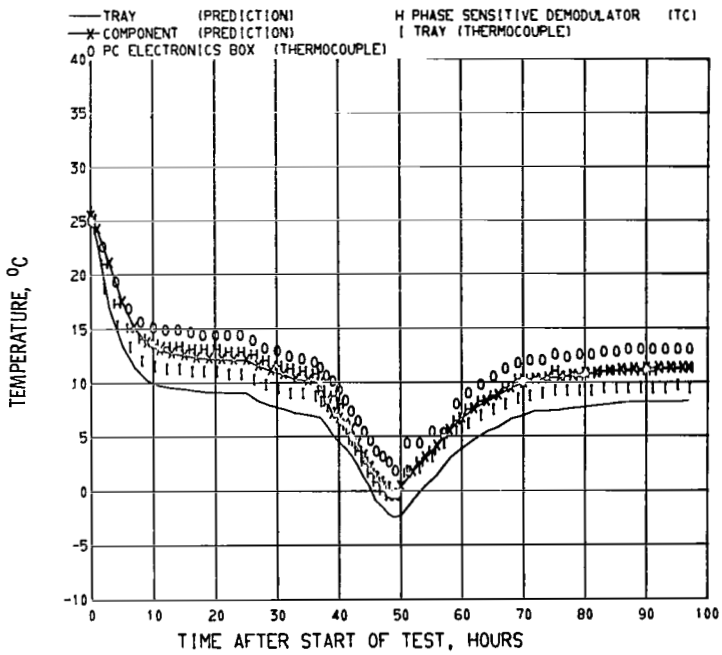

Figure 46. - Spacecraft support unit bay 6 lower area.

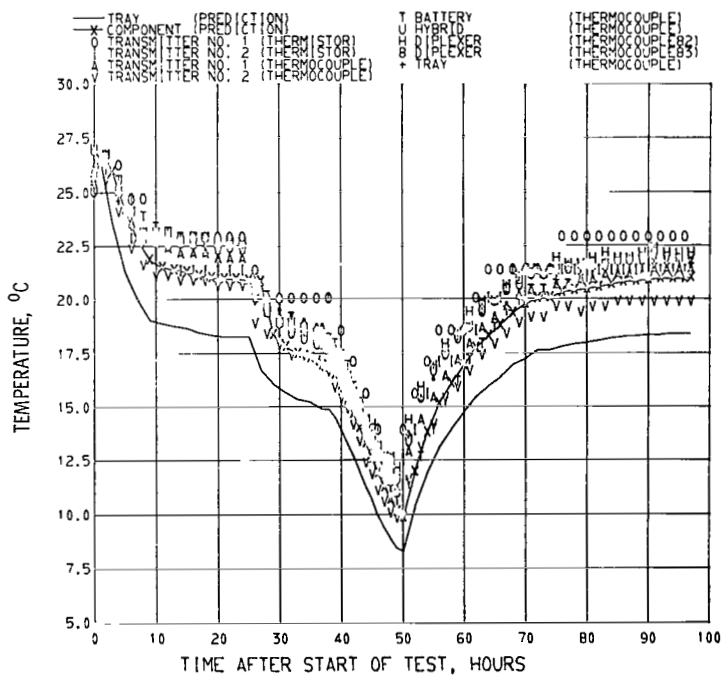

Figure 47. - Spacecraft support unit bay 8.

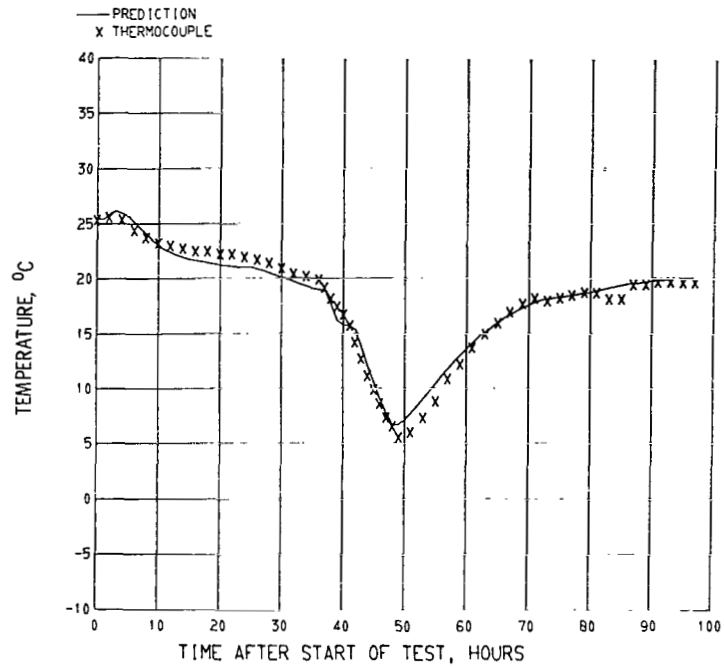

Figure 48. - Spacecraft support unit control moment gyro shelf.

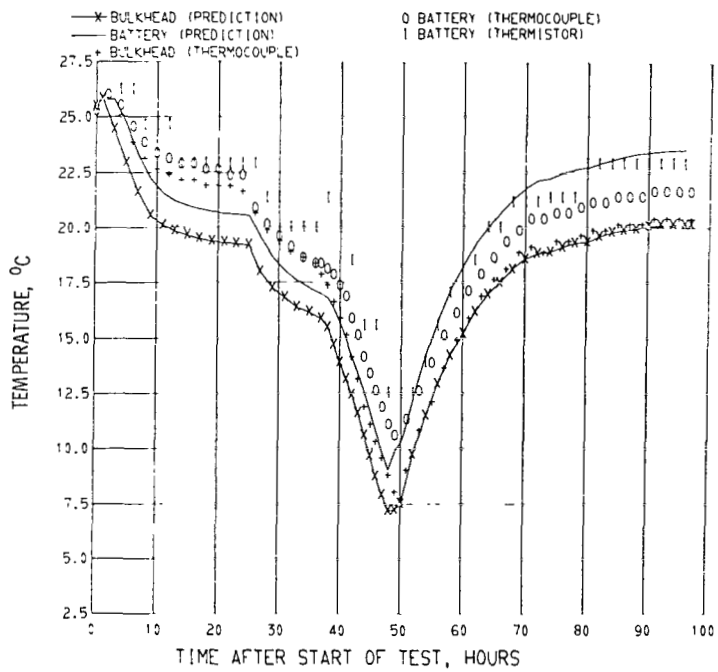

Figure 49. - Spacecraft support unit bay 8 battery.

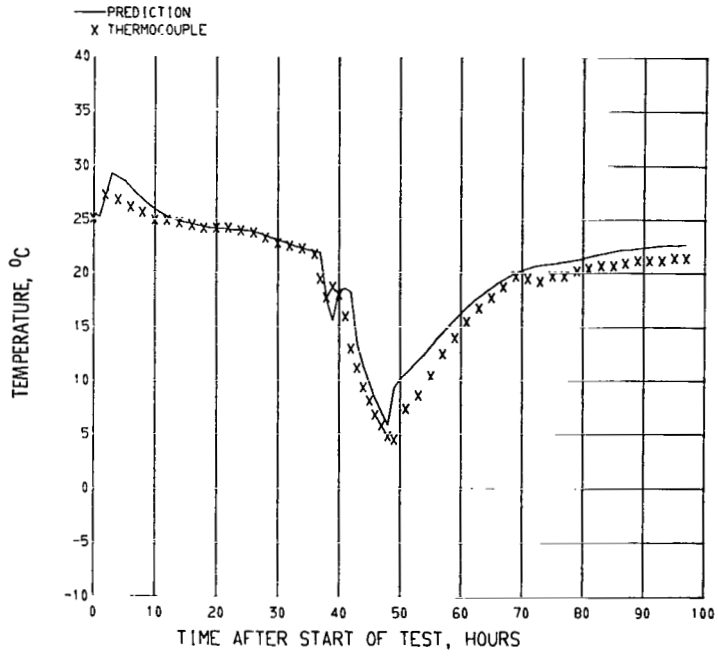

Figure 50. - Spacecraft support unit prototype control moment gyro (rear upper).

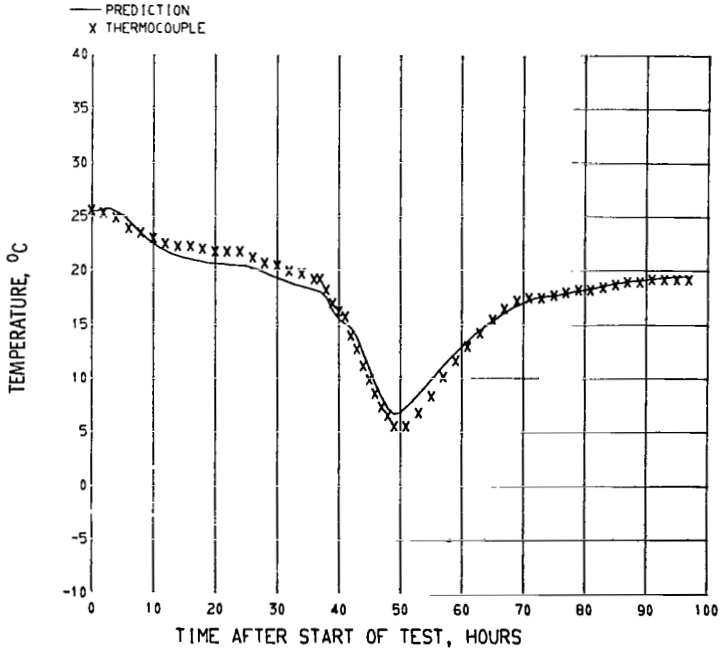

Figure 51. - Spacecraft support unit control moment gyro simulator (front upper).

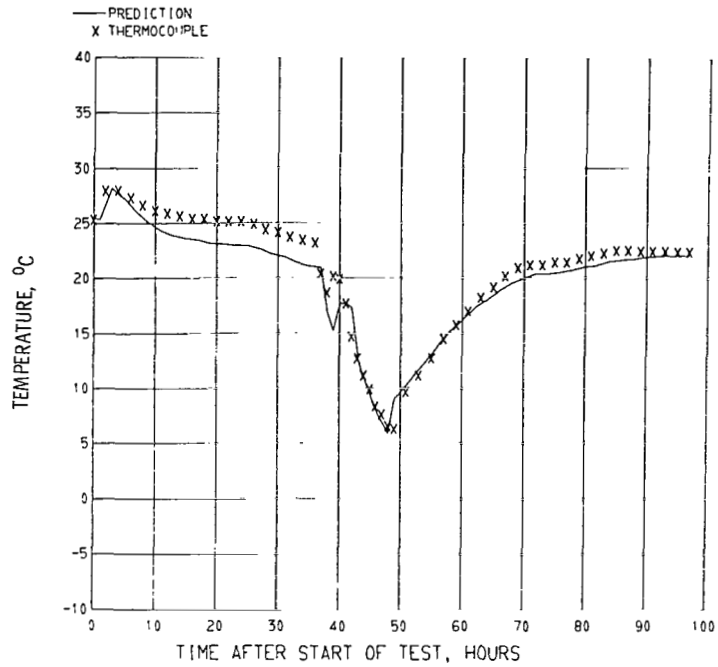

Figure 52. - Spacecraft support unit experimental control moment gyro (rear lower).

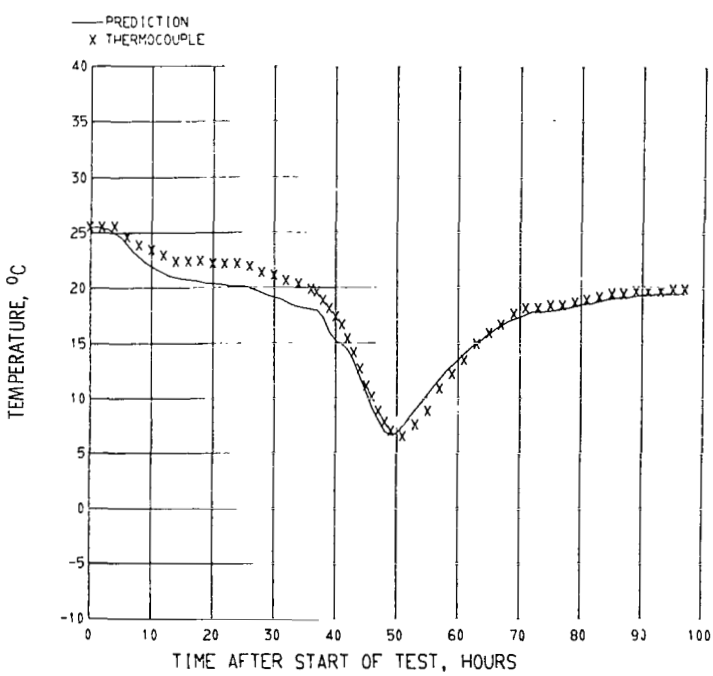

Figure 53. - Spacecraft support unit control moment gyro simulator front lower).

NASA-Langley, 1971 — 31 E-6396